

1 **PI3K γ is a molecular switch that controls immune suppression**

2

3 Megan M. Kaneda¹, Karen S. Messer^{1,2}, Natacha Ralainirina¹, Hongying Li^{1,2}, Chris
4 Leem¹, Sara Gorjestani¹, Gyunghwi Woo¹, Abraham V. Nguyen¹, Camila C.
5 Figueiredo^{1,3}, Philippe Foubert¹, Michael C. Schmid¹, Melissa Pink⁴, David G. Winkler⁴,
6 Matthew Rausch⁴, Vito J. Palombella⁴, Jeffery Kutok⁴, Karen McGovern⁴, Kelly A.
7 Frazer^{5,6}, Xuefeng Wu⁷, Michael Karin⁷, Roman Sasik⁸, Ezra E. W. Cohen^{1,9}, and Judith
8 A. Varner^{1,9,10,11}

9

10 Macrophages play critical, but opposite roles, in acute and chronic inflammation and
11 cancer¹⁻⁵. In response to pathogens or injury, inflammatory macrophages express
12 cytokines that stimulate cytotoxic T cells, while highly abundant macrophages in
13 neoplastic and parasitic diseases express anti-inflammatory cytokines that induce
14 immune suppression and may promote resistance to T cell checkpoint inhibitors¹⁻⁷. Here
15 we show that macrophage PI(3)Kinase γ controls a critical switch between immune
16 stimulation and suppression during inflammation and cancer. PI3K γ signaling through
17 Akt and mTor inhibits NF κ B activation while stimulating C/EBP β activation, thereby
18 inducing a transcriptional program that promotes immune suppression during
19 inflammation and tumor growth. In contrast, selective inactivation of macrophage PI3K γ
20 stimulates and prolongs NF κ B activation and inhibits C/EBP β activation, thus promoting
21 an immunostimulatory transcriptional program that restores CD8⁺ T cell activation and
22 cytotoxicity and synergizes with checkpoint inhibitor therapy to promote tumor
23 regression and extend survival in mouse models of cancer. As PI3K γ -directed, anti-

1 inflammatory gene expression predicted survival probability in cancer patients, our
2 findings demonstrate that therapeutic targeting of intracellular signaling pathways that
3 regulate the switch between macrophage polarization states can control immune
4 suppression in cancer and other disorders.

5

6 ¹Moore's Cancer Center, University of California, San Diego, La Jolla, CA, USA

7 ²Division of Biostatistics and Bioinformatics; Department of Family Medicine and Public
8 Health University of California, San Diego, La Jolla, CA, USA

9 ³Dep. Biologia Celular, UERJ, Rio de Janeiro, RJ, Brazil

10 ⁴Infinity Pharmaceuticals, Cambridge, MA

11 ⁵Department of Pediatrics, University of California, San Diego, La Jolla, California, USA

12 ⁶Institute for Genomic Medicine, University of California, San Diego, La Jolla, California,
13 USA

14 ⁷Department of Pharmacology, University of California, San Diego, La Jolla, CA, USA

15 ⁸Center for Computational Biology, Institute for Genomic Medicine, UCSD, USA

16 ⁹Department of Medicine, University of California, San Diego, La Jolla, CA, USA

17 ¹⁰Department of Pathology, University of California, San Diego, La Jolla, California, USA

18 ¹¹To whom correspondence should be addressed; 3855 Health Sciences Drive, La
19 Jolla, CA 92093-0819, tel: 858-822-0086; email: jvarner@ucsd.edu

20

21

1 We investigated the association between immune responses and survival in primary
2 tumors from HPV+ (n=97) and HPV- (n=423) head and neck squamous cell carcinoma
3 (HNSCC) cohorts from TCGA.⁸ High expression levels of pro-inflammatory mRNAs
4 *IL12A*, *IL12B*, *IFNG*, and *CD8A* were associated with increased survival in HPV+ but
5 not HPV- cohorts, while high expression of *IL6* was negatively associated with survival
6 (Extended Data Fig. 1a-e). HPV+ patients with this favorable immune expression profile
7 (n=35) had 97% survival at 3 years compared with 57% survival for patients without this
8 profile (n=62) (Fig. 1a). Similar associations were observed in lung adenocarcinoma and
9 gastric carcinoma patients (Extended Data Fig. 1f-g). These results suggested that
10 therapeutic approaches that stimulate pro-inflammatory gene expression might enhance
11 cancer patient survival.

12
13 We suspected that macrophage signaling pathways, such as those regulated by Class
14 IB isoform PI3K γ , might control the switch between immune stimulation and suppression
15 in inflammation and cancer. PI3K γ is abundantly expressed in myeloid but not cancer
16 cells (Extended Data Fig. 1h)⁹⁻¹² and promotes myeloid cell trafficking during
17 inflammation and cancer¹¹⁻¹⁵. Mice lacking PI3K γ (*p110 γ -/-*) mounted exaggerated,
18 macrophage-mediated pro-inflammatory responses upon exposure to pathogenic stimuli
19 (Fig. 1b; Extended Data Fig. 1i-k), suggesting that PI3K γ inhibits macrophage
20 inflammatory responses and might do so in the tumor microenvironment. Mice lacking
21 PI3K γ and mice that were treated with PI3K γ antagonists (TG100-115¹² or IPI-549¹⁶)
22 exhibited significantly suppressed growth of implanted HPV+ (MEER) and HPV-
23 (SCCVII) HNSCC, lung carcinoma (LLC), and breast carcinoma (PyMT) tumors (Fig.

1 1c). PI3K γ inhibition did not directly affect the growth or survival of tumor cells, which do
2 not express the kinase (Extended Data Fig. 1h, 1l-m)¹²⁻¹⁵. PI3K γ inhibition suppressed
3 long-term growth and metastases of spontaneous breast tumors, extended survival of
4 mice with orthotopic breast tumors and enhanced the sensitivity of tumors to the
5 nucleoside analogue gemcitabine (Fig. 1d; Extended Data Fig. 1n-q). While PI3K γ
6 inhibition did not affect the accumulation of CD11b+Gr1-F4/80+ tumor-associated
7 macrophages (TAMs) in tumors (Extended Data Fig. 2a-f), it enhanced expression of
8 MHCII and pro-inflammatory cytokines and inhibited expression of immune suppressive
9 factors in tumors and TAMs, indicating that PI3K γ controls the TAM switch between
10 immune suppression and immune stimulation (Fig. 1e-g Extended Data Fig. 2g-j, 3a-f).

11
12 To determine whether PI3K γ directly regulates macrophage polarization, we analyzed
13 mRNA and protein expression in primary murine macrophages stimulated in vitro with
14 basal (CSF-1), pro-inflammatory (IFN γ /LPS + CSF-1) or anti-inflammatory (IL-4 + CSF-
15 1) conditions. Pro-inflammatory stimuli upregulate macrophage expression of innate
16 immune proteins, cytokines and cell surface receptors, while anti-inflammatory stimuli
17 induces expression of immunosuppressive factors similar to those expressed in TAMs
18 (Extended Data Fig. 4a-c)¹. Genes and proteins associated with immune activation,
19 antigen-presentation and T cell activation were upregulated in *p110 γ ^{-/-}* and PI3K γ
20 inhibitor-treated macrophages (Fig. 2a-c, Extended Data Fig. 4c-f, 5a-g). In contrast,
21 genes associated with immune suppression and chemoattraction were inhibited (Fig.
22 2a-c, Extended Data Fig. 4c-f, 5a-g). These results confirm that PI3K γ controls a
23 macrophage switch between immune stimulation and suppression.

1
2
3
4
5
6
7
8
9
10
11
12
13
14
15
16
17
18
19
20
21
22

To identify how PI3K γ regulates macrophage immune responses, we evaluated DNA binding activities of NF κ B p65 RelA and the C/CAAT enhancer binding protein C/EBP β in WT and *p110 γ* null macrophages, as NF κ B promotes expression of inflammatory cytokines¹⁷, while C/EBP β promotes expression of the immunosuppressive factor *Arg1*.¹⁸⁻¹⁹ PI3K γ ablation rapidly and sustainably stimulated RelA DNA binding activity in macrophages (Fig. 2d, Extended Data Fig. 5h). In contrast, PI3K γ ablation suppressed DNA binding activity of C/EBP β (Fig. 2e). Consistent with these findings, PI3K γ inhibition stimulated and sustained p65 RelA phosphorylation and simultaneously inhibited C/EBP β and Akt phosphorylation (Fig. 2f-g, Extended Data Fig. 6a-b).

We next examined the effect of PI3K γ inhibition on the stability and phosphorylation of proteins that activate NF κ B, including the TLR4-associated adaptor protein IRAK-1 and inhibitory kappa B kinase β , IKK β , which promotes degradation of I κ B α , with subsequent release of NF κ B from an inhibitory I κ B-NF κ B complex¹⁷. PI3K γ deletion enhanced phosphorylation of IKK β and TBK1 and degradation of IRAK-1 and I κ B α in LPS-stimulated *p110 γ* ^{-/-} macrophages (Fig. 2h). As an IKK β inhibitor suppressed the inflammatory phenotype observed in *p110 γ* ^{-/-} macrophages (Fig. 2i), these results indicate PI3K γ is both a feedback inhibitor of the TLR4-NF κ B activation pathway and a promoter of IL-4 and C/EBP β signaling.

1 C/EBP β has been previously linked with tumor immune suppression through its control
2 of *Arg-1* expression¹⁸⁻¹⁹. Expression of constitutively activated PI3K γ (*p110 γ CAAX*)¹¹
3 was sufficient to induce *Arg-1* expression, in a manner that was inhibited by *Cebpb*,
4 *Mtor*, or *S6ka* knockdown (Extended Data Fig. 6c-d). *Cebpb* knockdown as well as
5 inhibitors of S6K and mTOR suppressed expression of immune suppressive factors and
6 stimulated expression of pro-inflammatory cytokines (Extended Data Fig. 6e-g). These
7 results show that PI3K γ promotes immune suppression by activating mTor-S6K α -
8 C/EBP β and inhibiting NF κ B, thereby controlling a switch that regulates the balance
9 between immune suppression and stimulation.

10

11 Since PI3K γ blockade stimulates pro-inflammatory responses in macrophages, we
12 asked whether macrophage PI3K γ blockade promotes adaptive immunity. TAMs were
13 isolated from WT and *p110 γ ^{-/-}* tumors, mixed with tumor cells and adoptively transferred
14 into new WT or *p110 γ ^{-/-}* recipient mice (Fig. 3a). Tumor growth was significantly
15 inhibited in tumors containing *p110 γ ^{-/-}* TAMs but not WT TAMs (Fig. 3b). CD8⁺ T cells
16 were significantly increased in tumors with *p110 γ ^{-/-}* but not WT macrophages (Fig. 3c,
17 Extended Date Fig. 6h), indicating that PI3K γ signaling in TAMs inhibits CD8⁺ T cell
18 recruitment to tumors. To determine whether macrophage-derived cytokines control
19 tumor growth, we implanted tumor cells mixed with in vitro cultured macrophages or
20 conditioned medium (CM) into WT mice. Tumor growth was enhanced by IL-4
21 stimulated WT macrophages and CM but inhibited by IL-4 stimulated *p110 γ ^{-/-}*
22 macrophages and CM from *p110 γ ^{-/-}* or PI3K γ inhibitor-treated macrophages and by all
23 LPS-stimulated macrophages and CM (Fig. 3d-e). To determine which macrophage-

1 derived immune factors affect tumor growth in vivo, we treated WT and *p110γ*^{-/-} TAMs
2 ex vivo with inhibitors of mTor, Arginase, IKKβ, IL-12 or NOS2 prior to mixing with tumor
3 cells and implanting in mice (Extended Data Fig. 6i). Blockade of mTOR or Arginase in
4 WT macrophages suppressed tumor growth, while inhibition of NOS2, IL-12 or IKKβ in
5 *p110γ*^{-/-} macrophages stimulated tumor growth. These results indicate that PI3Kγ-
6 mTOR mediated immune suppression promotes tumor growth and that PI3Kγ inhibition
7 reverses these effects by shifting macrophages toward NFκβ-dependent pro-
8 inflammatory polarization.

9

10 To confirm that *macrophage* PI3Kγ controls tumor growth, mice bearing pre-established
11 tumors were treated with PI3Kγ inhibitors in combination with clodronate liposomes,
12 which deplete macrophages from tissues.²⁰ PI3Kγ inhibitor and clodronate liposome
13 treatment each partially inhibited tumor growth and stimulated T cell recruitment, but the
14 combination had no additive effects, confirming that PI3Kγ in macrophages, rather than
15 other cell types, promotes tumor growth (Extended Data Fig. 7a-d). Similar results were
16 noted when CSF1R inhibition²¹ and PI3Kγ inhibition were combined (Extended Data Fig.
17 7e-f).

18

19 PI3Kγ blockade stimulated T cell recruitment into tumors, as total and CD8⁺ T cell
20 content increased in tumors from *p110γ*^{-/-} mice without significantly altering systemic T
21 cell content (Fig. 3f; Extended Data Fig. 7g-i). PI3Kγ inhibition did not suppress tumor
22 growth in CD8 null or antibody-depleted mice, suggesting PI3Kγ inhibition blocks tumor

1 growth by recruiting and/or activating CD8⁺ T cells (Fig. 3g, Extended Data Fig. 7j-k).
2 When T cells were isolated from tumor-bearing or naive animals, mixed with tumor cells
3 and implanted in mice, only T cells from *p110γ^{-/-}* tumor-bearing animals suppressed
4 tumor growth (Fig. 3h). However, PI3K γ inhibition did not directly activate T cells, as
5 neither PI3K γ deletion nor treatment of T cells with PI3K γ inhibitors ex vivo affected T
6 cell proliferation or activation; in contrast, PI3K δ inhibition suppressed T cell activation in
7 vitro and promoted tumor growth in vivo (Fig. 3i; Extended Data Fig. 7l-m, 8a-b). PI3K γ
8 inhibition promoted T cell mediated cytotoxicity, as T cells isolated from *p110γ^{-/-}* or
9 PI3K γ inhibitor-treated tumors stimulated tumor cell cytotoxicity (Extended Data Fig. 8c-
10 g). T cells from *p110γ^{-/-}* or PI3K γ inhibitor-treated animals expressed significantly more
11 IFN γ and Granzyme B and significantly less TGF β 1 and IL10 protein and mRNA than T
12 cells from WT animals (Fig. 3j; Extended Data Fig. 8h-l). Together, these results
13 indicate that macrophage PI3K γ inhibition indirectly promotes both Th1 and cytotoxic
14 adaptive immune responses.

15
16 To determine whether PI3K γ inhibition interacts with other immune therapies, we
17 combined PI3K γ and the checkpoint inhibitor anti-PD-1 in mouse tumor models. PD-L1,
18 but not PD-L2, was expressed on macrophages in vitro and in vivo (Extended Data Fig.
19 9a-b). PI3K γ inhibition synergized with anti-PD-1 to suppress the growth of HPV+
20 HNSCC tumors in *p110γ^{-/-}* or inhibitor-treated male or female animals, inducing tumor
21 regression in 86% of male and 90-100% of female animals, as well as continuous
22 survival to date in 60% of male mice and 90-100% of female mice (Fig. 4a-c, Extended
23 Data Fig. 9c-d). Importantly, PI3K γ inhibition also synergized with anti-PD-1 to reduce

1 tumor growth, extending survival and inducing tumor regression in 30% of mice bearing
2 HPV- HNSCC (SCCVII) tumors (Fig. 4d-f, Extended Data Fig. 9e). The combination of
3 PI3K γ and anti-PD-1 inhibitors activated T cell memory, as 100% of mice that had
4 previously cleared HPV+ tumors efficiently suppressed re-challenge with HPV+ tumor
5 cells and remained cancer free (Extended Data Fig. 9f). PI3K γ and PD-1 inhibitors each
6 stimulated immune response gene expression and inhibited immune suppressive gene
7 expression, MHCII expression in TAMs, and CD8+ T cell recruitment to tumors;
8 combination therapy further elevated these parameters (Fig. 4g-i, Extended Data Fig.
9 9g). These studies show that PI3K γ inhibition can synergize with T cell targeted therapy
10 to promote anti-tumor immune responses that induce sustained tumor regression in
11 murine models of cancer.

12

13 PI3K γ -regulated immune responses might also affect outcome in cancer patients. We
14 identified 43 PI3K γ -regulated genes that significantly associated with survival in TCGA
15 HPV+ HNSCC patients (Fig. 5j). HPV+ HNSCC patients with a low PI3K γ activity profile
16 experienced 100% survival at 3 years, compared with 56% survival for the remaining 63
17 patients (Fig. 5k). In HPV- HNSCC patients, 39 of these genes were significantly shifted
18 in the direction of high PI3K γ activity, consistent with a pattern of pervasive immune
19 suppression and reduced survival in HPV- disease (Extended Data Fig. 10a). In lung
20 adenocarcinoma patients, 18 genes predicted survival; patients with a low PI3K γ
21 activity profile had 73% survival at 3 years, compared with 55% survival for others
22 (Figure 5l). These results suggest that a PI3K γ -regulated immune suppression signature

1 is associated with survival in cancer patients and that PI3K γ inhibitors might provide
2 clinical benefit in cancer patients.

3

4 Here we have shown that PI3K γ regulates innate immunity during inflammation and
5 cancer (Extended Data Fig.10b-c). Prior studies have implicated PI3Ks in the regulation
6 of pro-inflammatory immune responses in macrophages, as pan-PI3K inhibitors and null
7 mutations in the PI3K γ effectors PDK1, Akt1 and TSC enhanced pro-inflammatory NF κ B
8 dependent transcription in macrophages,²²⁻²⁴ while inhibition of PTEN and SHIP, which
9 oppose PI3Kinase function, promotes immune suppression.²⁵⁻²⁶ As macrophage
10 reprogramming can enhance the activity of checkpoint inhibitors in cancer^{5,13,21,27}, our
11 studies indicate that inhibitory targeting of macrophage signaling pathways may provide
12 novel approaches to improve the long-term survival of cancer patients.

13

14 **Online content**

15 Supplementary data display items are available in the online version of the paper. For
16 gel source data see Supplementary Figure 1.

17

18 **Acknowledgements**

19 This work was supported by NIH grants R01CA126820 (JAV), T32HL098062 (MMK),
20 T32CA009523 (SG) and T32CA121938 (SG), the CAPES Foundation and Ministry of
21 Education of Brazil (CF) and by Ralph and Fernanda Whitworth and the Immunotherapy
22 Foundation (JAV and EEC). The authors thank John Lee and Stephen Schoenberger
23 for HPV+MEER HNSCC and SSCVII cells.

1

2 **Author contributions**

3 TCGA analysis was performed by HY and KSM, RNA sequencing by KAF, MMK, SG,
4 and RS, flow cytometry by MMK and NR, in vitro studies by MMK, NR, SG, GW, CCF,
5 AVN, MCS, and animal studies by MMK, NR, CL and PF. MP, VJP, JK, KM, MR and
6 DGW provided IPI-549 and Fig.1c, Extended Data Fig. 8a-b. ML120B was contributed
7 by XW and MK. The project was directed by EEWC, KSM and JAV. The manuscript
8 was written by JAV and MMK.

9

10 **Author information**

11 Data deposition: RNA sequencing data can be accessing using numbers GSE58318
12 and GSE84318 at www.ncbi.nlm.nih.gov/geo. Reprints and permissions information is
13 available at www.nature.com/reprints.The authors declare competing financial interests:
14 details accompany the full-text HTML version of the paper. Correspondence and
15 requests for materials should be addressed to jvarner@ucsd.edu.

1 **Figure 1: PI3K γ promotes immune suppression.** (a) Multivariate immune response
2 mRNA signature in HPV+ HNSCC patients (n=97). (b) Immune response mRNA
3 expression in p110 γ ^{-/-} or WT peritoneal macrophages (n=3). (c) Mean +/- sem tumor
4 growth in WT, p110 γ ^{-/-} and PI3K γ -inhibitor-treated mice (n=15). Arrow, daily treatment
5 initiation. (d-f) Mean +/- sem (d) spontaneous breast carcinoma growth and metastasis
6 (bar, 200 μ m) in WT (n=21) and p110 γ ^{-/-} (n=8) animals; (e) MHCII expression on WT vs
7 p110 γ ^{-/-} TAMs (n=3) and (f) fold change mRNA expression in tumors and tumor-derived
8 CD11b⁺ cells from p110 γ ^{-/-} and PI3K γ inhibitor-treated mice (n=5). (g) Heatmap of
9 immune response mRNA expression in tumors from WT and p110 γ ^{-/-} mice (n=3).
10 n=biological replicates.

11

12 **Figure 2: PI3K γ regulates NF κ B and C/EBP β during macrophage polarization.** (a)
13 Heatmap of mRNA expression in p110 γ ^{-/-} vs WT macrophages (n=3). (b-c) Mean +/-
14 sem (b) mRNA (n=3) and (c) protein (n=4) expression. (d-e) Mean +/- sem (d) p65 RelA
15 and (e) C/EBP β DNA-binding activity in WT and p110 γ ^{-/-} macrophages (n=4). (f-g)
16 Immunoblotting of pRelA/RelA, pC/EBP β /C/EBP β , and pAkt/Akt in (f) LPS and (g) IL-4
17 stimulated WT and p110 γ ^{-/-} macrophages. (h) Immunoblotting of IRAK1, pIKK β /IKK β ,
18 I κ B α , pTBK1/TBK1, p110 γ and actin in WT and p110 γ ^{-/-} macrophages. (i) Mean +/- sem
19 mRNA expression in IKK β inhibitor-treated macrophages (n=3). n=biological replicates.

20

21 **Figure 3: Macrophage PI3K γ suppresses T cell activation.** (a) Adoptive transfer
22 method. (b) Weights of tumors implanted with p110 γ ^{-/-}, WT or no TAMs (n=8). (c) CD8⁺

1 T cells from b (n=16). (d, e) Weights of tumors implanted with (d) in vitro cultured
2 macrophages (n=8) or (e) macrophage-conditioned medium (CM) (n=8). (f) Percent T
3 cells in WT and p110 γ ^{-/-} tumors (n=3). (g) Tumor volumes in p110 γ and/or CD8^{-/-} mice
4 (n=6). (h-i) Weights of tumors implanted with (h) naïve or tumor-derived T cells (n=8) or
5 (i) inhibitor-treated T cells (n=16). (j) IFN γ and Granzyme B expression in tumors and T
6 cells from WT and p110 γ ^{-/-} animals (n=3). All graphs show mean +/- sem of biological
7 replicates.

8

9 **Figure 4: PI3K γ inhibition synergizes with anti-PD-1.** (a, d) Mean +/- sem tumor
10 volumes in anti-PD-1 (black arrows) treated (a) WT or p110 γ ^{-/-} mice with HNSCC HPV+
11 tumors (n=13) and (d) PI3K γ inhibitor-treated mice with HPV- HNSCC tumors (n=13). (b,
12 e) Percent survival of mice in a, d. (c, f) Change in tumor volumes in a, d. (g-h)
13 Heatmap (g) and graph (h) of mRNA expression from d (n=3). (i) Immune cell profiles
14 from d. (j) Heatmap of PI3K γ -regulated mRNA expression in HPV+HNSCC patients
15 (n=45). (k-l) Multivariate PI3K γ -regulated immune signature in (k) HPV+HNSCC patients
16 (n=97) and (l) lung adenocarcinoma patients (n=507). n=biological replicates.

1 **METHODS**

2

3 **Immune-related gene expression signature analysis in TCGA data**

4 We analyzed TCGA data for association between mRNA expression level of
5 sixteen candidate immune-related genes (*ARG1, IL10, FOXP3, CD68, IL12A, IL12B,*
6 *IFNG, CD8A, CD4, CD11B, CD14, TNFA, IL1A, IL1B, IL6* and *CCL5*) and 5-year overall
7 survival. Illumina HiSeq RNAseqV2 mRNA expression and clinical data for 520 Head
8 and Neck squamous cell carcinoma samples were downloaded from the TCGA data
9 portal. Median follow-up from diagnosis was 1.8 years with range 0.01 years to 17.6
10 years. Follow-up time was truncated at 5-years for analysis and 200 deaths occurred
11 in this period. For each of the 16 candidate immune response genes, we scored
12 subjects as above (high) or below (low) the median expression and compared survival
13 using a log rank test at 5% significance. HPV+ patients were stratified into a favorable
14 immune profile if they had expression above the median for the significant genes *IL12A,*
15 *IL12B IFNG, CD8A* and below the median for *IL6*. Kaplan-Meier curves were plotted for
16 these two groups. Similar methods were used to examine association of these 16 genes
17 with 720 lung adenocarcinoma, and 876 gastric carcinoma samples using the publically
18 available data from KM Plotter²⁸. In lung adenocarcinoma, 12 genes were significantly
19 associated with survival; patients were scored as having a favorable immune profile if 7
20 or more of the 12 significant genes had expression in the favorable direction. In 876
21 gastric cancer samples, 8 genes were significantly associated with survival. patients
22 were scored as having a favorable immune profile if 5 out of the 8 genes had
23 expression in the favorable direction.

1
2
3
4
5
6
7
8
9
10
11
12
13
14
15
16
17
18
19
20
21
22
23

PI3K γ -regulated gene expression signature analysis in TCGA data

We investigated 66 immune-related genes in four functional classes (17 genes related to antigen presentation (HLA class I and II molecules), 24 genes surveying T cell activation, 20 innate immune response genes (*IL6*, *CCL7* and others), and 5 genes related to cancer cell signaling) that changed expression in response to PI3K γ inhibition for association with survival in HPV+ and HPV- TCGA HNSCC and lung adenocarcinoma cohorts. Within each cancer type, we scored subjects as above or below the median expression for each gene and compared survival using a log rank test, using 10% FDR within each class as the significance threshold. HPV+ and HPV- HNSCC survival were investigated separately, as HPV- HNSCC has generally worse prognosis. Within each cohort, patients were classified as having a favorable PI3K γ immune response profile if they had expression levels above or below the median in the direction of low PI3K γ activity for the genes identified as significant. We compared the survival experience of favorable vs less-favorable patients using Kaplan-Meier curves. Out of the 66 experimentally identified PI3K γ regulated genes 43 showed significant association with overall survival in the HPV+ cohort (FDR<10% within each functional class). Comparison of these genes between HPV+ and HPV- cohort showed that HPV- samples generally had significantly ($p<0.05$) lower expression of 42 genes in the antigen presentation and T cell activation classes, consistent with a pattern of adaptive immune suppression, and higher expression of genes in the innate immune response and cancer cell signaling class, which were negatively associated with survival. Only Malt1 was not differentially expressed between the two groups ($p=0.7$).

1

2 **Mice**

3 *Pik3cg*^{-/-} (*p110γ*^{-/-}) and *Pik3cg*^{-/-}; PyMT animals were generated as previously
4 described¹². *Cd8*^{-/-} and *Cd4*^{-/-} animals in the C57Bl6 background were purchased from
5 the Jackson Laboratory, Bar Harbor, ME and crossed with syngeneic *Pik3cg*^{-/-} animals.
6 All animal experiments were performed with approval from the Institutional Animal Care
7 and Use Committee of the University of California, San Diego, La Jolla, CA. Animal
8 were euthanized before the maximum IACUC allowable tumor burden of 2 cm³/mouse
9 was exceeded.

10

11 **Tumor studies**

12 Wildtype or *p110γ*^{-/-} 6-8 week-old female or male syngeneic C57Bl/6J (LLC lung,
13 PyMT breast, and MEER HPV+ HNSCC) or C3He/J (SSCVII HPV- HNSCC) mice were
14 implanted with 1x10⁶ tumor cells by subcutaneous injection (LLC, MEER, SCCVII) or by
15 orthotopic injection (PyMT) (n=10-15) and tumor growth was monitored for up to 30
16 days. Tumor dimensions were measured once when tumors were palpable. Tumor
17 volumes were calculated using the equation ($l^2 \times w$)/2. In some studies, WT and *p110γ*^{-/-}
18 animals with LLC tumors were treated with gemcitabine (150 mg/kg) or saline by i.p
19 injection on d7 and d14 (n=10). LLC were acquired from ATCC, PyMT were from Lesley
20 Ellies (University of California, San Diego), HPV+ MEER were from John Lee (Cancer
21 Biology Research Center, Sanford Research/USD, Sioux Falls, SD) and SCCVII
22 squamous carcinoma cells were from Stephen Schoenberger (La Jolla Institute for
23 Allergy and Immunology). All cell lines were tested for mycoplasma and mouse

1 pathogens and checked for authenticity against the International Cell Line
2 Authentication Committee (ICLAC; <http://iclac.org/databases/cross-contaminations/>) list.

3 In some studies, mice bearing LLC, PyMT, HPV+ MEER or HPV- HNSCC tumor
4 cells were treated once daily by oral gavage with vehicle (5%NMP/95% PEG 400),
5 15mg/kg/day of the PI3K γ inhibitor IPI-549 or by i.p. injection with 2.5 mg/kg b.i.d of
6 TG100-115^{9,43} beginning on day 8 post-tumor injection and continuing daily until
7 sacrifice. IPI-549 is an orally bioavailable PI3K γ inhibitor with a long plasma half-life and
8 a KD value of 0.29 nM for PI3K γ with >58-fold weaker binding affinity for the other Class
9 I PI3K isoforms²⁶. Enzymatic and cellular assays confirmed the selectivity of IPI-549 for
10 PI3K γ (>200-fold in enzymatic assays and >140-fold in cellular assays over other Class
11 I PI3K isoforms²⁶. To study the effect of IPI-549 on lung tumor growth, LLC tumor cells
12 were passaged three times in C57/BL6 Albino male mice. When tumor volume reached
13 1500 mm³, tumors were harvested and single-cell suspensions were prepared. This
14 tumor brei inoculum was implanted subcutaneously in the hind flank of C57/BL6 Albino
15 male mice at 1x10⁶ cells/ mouse. Prior to initiating treatment with once daily IPI-549 (15
16 mg/kg p.o.), groups were normalized on the basis of tumor volume. In some studies,
17 WT and *p110 γ* ^{-/-} tumor-bearing mice were treated with 100 μ g of anti-CD8 (clone YTS
18 169.4) or isotype control clone (LTF-2) from BioXCell administered by i.p. injections on
19 day 7, 10 and 13 of tumor growth. For all tumor experiments, tumor volumes and
20 weights were recorded at sacrifice.

21

22 **Anti-PD-1 tumor studies**

1 C57Bl/6J (wildtype) or *p110γ*^{-/-} 6-8 week-old male or female mice (MEER HPV+
2 HNSCC) or C3He/J (SCCVII HPV- HNSCC) were implanted with tumor cells by
3 subcutaneous injection (1×10^6 MEER or 1×10^5 SCCVII). In HPV+ MEER studies,
4 wildtype and *p110γ*^{-/-} animals were treated with 4 doses of 250 μg of anti-PD-1 antibody
5 (Clone RMP-14, Bioxcell) or Rat IgG2a isotype control (Clone2A3, Bioxcell) every 3
6 days starting when tumors became palpable on day 11 (n = 12-14 mice per group).
7 Wildtype mice bearing HPV+ tumors were also treated with the p110γ inhibitor TG100-
8 115⁴³ b.i.d. by i.p. injection, beginning on day 11. Tumor regressions were calculated as
9 a percentage of the difference in tumor volume between the date treatment was initiated
10 and the first date of sacrifice of the control group. For HPV-SCCVII studies, C3He/J
11 mice were treated with PI3Kγ inhibitor (2.5mg/kg TG100-115 i.p.) beginning on day 6
12 post-tumor inoculation and with 6 doses of anti-PD-1 antibody (250μg Clone RMP-14,
13 Bioexcell) or Rat IgG2a isotype control Clone 2A3, Bioxcell) every 3 days beginning on
14 day 3 (n=12 mice per group) or with a combination of the two. Alternatively, mice were
15 treated with 5mg/kg TG100-115 b.i.d. +/- anti-PD-1 (250μg every 3 days) beginning on
16 day 1 (Figure 4). Mice that completely cleared HPV+ MEER tumors were re-injected
17 with HPV+ tumor cells contralateral to the initial tumor injection and tumor growth was
18 monitored.

19

20 **PyMT models of mammary carcinoma**

21 The growth and metastasis of spontaneous mammary tumors in female PyMT+ (n=13)
22 and *p110γ*^{-/-} PyMT+ (n=8) animals was evaluated over the course of 0-15 weeks. Total
23 tumor burden was determined by subtracting the total mammary gland mass in PyMT-

1 animals from the total mammary gland mass in PyMT+ animals. Lung metastases were
2 quantified macroscopically and microscopically in H&E tissue sections at week 15.

3

4 **LPS induced septic shock**

5 Septic shock was induced in WT and p110 γ ^{-/-} mice via intraperitoneal injection of 25
6 mg/kg LPS (Sigma, B5:005). Survival was monitored every 12h and liver, bone marrow
7 and serum were collected 24h post LPS injection.

8

9 **Macrophage depletion studies**

10 C57Bl/6J female mice were implanted with 1×10^6 LLC tumor cells by subcutaneous
11 injection. When the average tumor size was 250 mm³, mice were treated by i.p.
12 injection with 1 mg/mouse clodronate or control liposomes (Clodronateliposomes.com,
13 Amsterdam, The Netherlands) every 4 days for 2 weeks in combination with daily
14 administration of vehicle or IPI-549 (15 mg/kg/day p.o.). In other studies, six week old
15 female BALB/c mice were injected subcutaneously with 2.5×10^5 CT26 murine colon
16 carcinoma cells in 100 μ l PBS into the right flank. Eight days later, tumor-bearing mice
17 were arranged into four groups (n=15) with an average tumor volume of 70mm³. Oral
18 administration of IPI-549 (15mg/kg) or Vehicle (5%NMP/95% PEG 400) and anti-CSF-
19 1R antibody (50mg/kg i.p. 3x per week, Clone AFS98, Bioexcell) began on day 8 post-
20 tumor injection via gavage at a 5 mL/kg dose volume and continued daily for a total of
21 18 doses.

22

23 **Tumor infiltrating myeloid cell analysis**

1 Six week old female BALB/c mice were injected subcutaneously with 2.5×10^5 CT26
2 murine colon carcinoma cells in 100 μ l PBS into the right flank. On day 8 post tumor
3 injection, tumor-bearing animals were grouped and treated with IPI-549 (15 mg/kg, QD,
4 PO) or Vehicle (5%NMP/95% PEG 400). In addition, mice were injected i.p. with
5 50mg/kg anti-CD115 (BioXcell Clone: AFS98 Cat: BE0213) or 50mg/kg rat IgG2a
6 isotype control (BioXcell Clone: 2A3 Cat: BE0089-R005) antibodies as described above
7 for a total of three injections. Two days after the final injection animals were euthanized,
8 tumors were digested in a mixture of 0.5 mg/ml Collagenase IV and 150 U/ml DNase I
9 in RPMI-1640 for 30 minutes at 37°C, and tumor-infiltrating myeloid cells were analyzed
10 by flow cytometry.

11

12 **In vivo macrophage adoptive transfer experiments**

13 CD11b+Gr1- cells were isolated from single cell suspensions of LLC tumors from donor
14 mice by FACS sorting or serial magnetic bead isolation. Additionally, for some
15 experiments, primary bone marrow derived macrophages were polarized and harvested
16 into a single cell suspension. Purified cells were admixed 1:1 with LLC tumor cells and 5
17 $\times 10^5$ total cells were injected subcutaneously into new host mice. Tumor dimensions
18 were measured 3 times per week beginning on day 7. In antibody blocking studies,
19 CD11b+Gr1- cells were incubated with 5 μ g of anti-IL-12 clone RD1-5D9 or isotype
20 clone LTF-2 (BioXCell) for 30 min prior to the addition of tumor cells. Mice were
21 additionally treated intradermally with 5 μ g of antibody 3 and 6 days after tumor cell
22 inoculation. In some studies, CD11b+Gr1- cells were pre-incubated with inhibitors of
23 Arginase (nor-NOHA, 50 μ M, Cayman Chemical), iNOS (1400W dihydrochloride, 100

1 μM , Tocris), mTOR (rapamycin, 10 μM Calbiochem), or IKK β (ML120B, 30 μM , Tocris)
2 for 30 min before the addition of tumor cells. Inoculated mice were further treated by
3 intradermal injection with inhibitors at 3 and 6 days post inoculation.

4

5 **T-cell adoptive transfer**

6 Donor C57Bl/6J (wildtype) or p110 $\gamma^{-/-}$ mice were implanted with 1×10^6 LLC tumor cells
7 by subcutaneous injection. On day 14 after tumor implantation, CD90.2+, CD4+ or
8 CD8+ cells were harvested by magnetic bead isolation (Miltenyi Biotec). T cells were
9 mixed 1:1 with viable LLC tumor cells. Cell mixtures containing 5×10^5 total cells were
10 injected into the flanks of naïve WT or p110 $\gamma^{-/-}$ mice (n=8-10 per group). Tumor growth,
11 intratumoral apoptosis and necrosis were investigated over 0-16 days. In other studies,
12 WT T cells were incubated at 37°C/5% CO₂ for 6h with 10 or 100 nM IPI-549 (Infinity
13 Pharmaceuticals) or Cal-101 (Selleck Chem). After 6h, T cells were washed, admixed
14 1:1 with LLC tumor cells, and 1×10^6 total cells were injected subcutaneously into
15 recipient mice. Tumor growth, was monitored for 14 days.

16

17 **Isolation of single cells from murine tumors**

18 Tumors were isolated, minced in a petri dish on ice and then enzymatically dissociated
19 in Hanks Balanced Salt Solution containing 0.5 mg/ml Collagenase IV (Sigma), 0.1
20 mg/ml Hyaluronidase V (Sigma), 0.6 U/ml Dispase II (Roche) and 0.005 MU/ml DNase I
21 (Sigma) at 37°C for 5-30 min. The duration of enzymatic treatment was optimized for
22 greatest yield of live CD11b+ cells per tumor type. Cell suspensions were filtered
23 through a 70 μm cell strainer. Red blood cells were solubilized with red cell lysis buffer

1 (Pharm Lyse, BD Biosciences, San Jose, CA), and the resulting suspension was filtered
2 through a cell strainer to produce a single cell suspension. Cells were washed one time
3 with PBS prior to use in flow cytometry analysis or magnetic bead purification.

4

5 **Peritoneal Macrophage Isolation**

6 Thioglycollate elicited peritoneal macrophages were collected 96h after i.p. injection of a
7 3% thioglycollate solution. Cells were harvested from the peritoneal cavity in 10ml of
8 PBS and macrophage enrichment was performed by plating cells in RPMI with 10%
9 FBS and 1% pen/strep for 2h at 37C 5% CO₂. After 2h, nonadherent cells were
10 removed with three PBS washes, and cells were analyzed via flow cytometry and qPCR
11 analysis.

12

13 **Flow cytometry staining and analysis**

14 Single cell suspensions (10⁶ cells in 100 μL total volume) were incubated with Aqua
15 Live Dead fixable stain (Life Technologies, Carlsbad, CA), FcR-blocking reagent (BD
16 Biosciences, San Jose, CA) and fluorescently labeled antibodies and incubated at 4°C
17 for 1h. Primary antibodies to cell surface markers directed against F4/80 (BM8), CD45
18 (30-F11), CD11b (M1/70), Gr1 (RB6-8C5), CD3 (145-2C11), CD4 (GK1.5), CD8 (53-
19 6.7), CD273 (B7-DC), CD274 (B7-H1) were from eBioscience; Ly6C (AL-21), Ly6G
20 (1A8), CD11c (HL3), and MHC-II (AF6-120.1) from BD Pharmingen, CCR2 (475301)
21 from R&D Systems and CD206 (MR5D3) from AbD Serotech. For intracellular staining,
22 cells were fixed, permeabilized using Transcription Factor Staining Buffer Set
23 (eBioscience) and then incubated with fluorescently labeled antibodies to FoxP3 (FJK-

1 16s) from eBioscience. Multicolor FACS Analysis was performed on a BD Canto RUO
2 11 Color Analyzer. All data analysis was performed using the flow cytometry analysis
3 program FloJo (Treestar).

4

5 **Magnetic bead purification of myeloid cells**

6 Single cell preparations from bone marrow or tumors were incubated with FcR-blocking
7 reagent (BD Biosciences) and then with 20 μ l magnetic microbeads conjugated to
8 antibodies against CD11b, Gr1, CD90.2, CD4 and CD8 (Miltenyi Biotech MACS
9 Microbeads)/1x10⁷ cells for 20 min at 4°C. Cells bound to magnetic beads were then
10 removed from the cell suspension according to manufacturers instructions.

11

12 **Flow cytometric sorting of cells from tumors and bone marrow**

13 For cell sorting, single cell suspensions were stained with Aqua Live Dead fixable stain
14 (Life Technologies) to exclude dead cells and anti-CD11b-APC (M1/70, eBioscience)
15 and anti-Gr1-FITC (RB6-8C5, eBioscience) antibodies. FACS sorting was performed on
16 a FACS Aria 11 color high speed sorter at the Flow Cytometry Core at the UC San
17 Diego Center for AIDS Research. Live cells were sorted into the following populations:
18 CD11b+Gr1⁻, CD11b+Gr1^{lo}, CD11b+Gr1^{hi} and CD11b-Gr1⁻ cells. CD11b positive cells
19 were defined by increased staining over the isotype control, and Gr1 levels were
20 defined both by comparison to the isotype control and relative staining to other
21 populations.

22

23 **Murine macrophage differentiation and culture**

1 Bone marrow derived cells (BMDC) were aseptically harvested from 6-8 week-old
2 female mice by flushing leg bones of euthanized mice with phosphate buffered saline
3 (PBS), 0.5% BSA, 2mM EDTA, incubating in red cell lysis buffer (155 mM NH₄Cl, 10
4 mM NaHCO₃ and 0.1 mM EDTA) and centrifuging over Histopaque 1083 to purify the
5 mononuclear cells. Approximately 5X10⁷ BMDC were purified by gradient centrifugation
6 from the femurs and tibias of a single mouse. Purified mononuclear cells were cultured
7 in RPMI + 20% serum + 50ng/ml M-CSF (PeproTech).

8

9 **Human macrophage differentiation and culture**

10 Human leukocytes concentrated by from apheresis were obtained from the San Diego
11 Blood Bank. Cells were diluted in phosphate buffered saline (PBS), 0.5% BSA, 2mM
12 EDTA, incubated in red cell lysis buffer (155 mM NH₄Cl, 10 mM NaHCO₃ and 0.1 mM
13 EDTA) and centrifuged over Histopaque 1077 to purify mononuclear cells.
14 Approximately 10⁹ BMDC were purified by gradient centrifugation from one apheresis
15 sample. Purified mononuclear cells were cultured in RPMI + 20% serum + 50ng/ml
16 Human M-CSF (PeproTech). Non-adherent cells were removed after 2h by washing,
17 and adherent cells were cultured for 6 days to differentiate macrophages fully.

18

19 **Macrophage polarization**

20 Bone marrow derived macrophages were polarized with either IFN_γ (20 ng/ml,
21 Peprotech) plus LPS (100 ng/ml, Sigma) or LPS alone for 24h or IL-4 (20 ng/ml,
22 Peprotech) for 24-48h. For inhibitor studies, PI3K_γ inhibitors (1 μM) (IPI-549, Infinity
23 Pharmaceuticals and TG100-115, Targegen/Sanofi-Aventis), rapamycin (10 μM)

1 (Selleck), or ML120B (30 μ M) were incubated with macrophages 1h prior to the addition
2 of polarizing stimuli. Total RNA was harvested from macrophages using the RNeasy
3 Mini Kit (Qiagen) according to the manufacture's instructions.

4

5 **RNA sequencing**

6 Freshly isolated mouse bone marrow cells from 9 WT and 9 p110 γ ^{-/-} mice were pooled
7 into 3 replicates sets of WT or p110g^{-/-} cells and differentiated into macrophages for six
8 days in RPMI + 20% FBS+ 1%Pen/Strep+ 50 ng/ml M-CSF. Each replicate set of
9 macrophages was then treated with mCSF, IL-4 or IFNg/LPS. Macrophages were
10 removed from dishes, and RNA was harvested using Qiagen Allprep kit. In addition,
11 RNA was harvested from day 14 (500mm³) LLC tumors or purified CD11b+Gr1-F480+
12 TAMs from WT (C57BL/6) and p110 γ ^{-/-} null mice. RNA was harvested using Qiagen
13 Allprep kit. RNA libraries prepared from 1 μ g RNA per sample were prepared for
14 sequencing using standard Illumina protocols. RNA sequencing was performed by the
15 University of California, San Diego Institute for Genomic Medicine. mRNA profiles were
16 generated by single read deep sequencing, in triplicate, using Illumina HiSeq2000.

17

18 **Sequence analysis**

19 Sequence analysis was performed as previously described.¹⁵ Sequence files from
20 Illumina HiSeq that passed quality filters were aligned to the mouse transcriptome (mm9
21 genome build) using the *Bowtie2* aligner⁴. Gene-level count summaries were analyzed
22 for statistically significant changes using *DESeq*. Individual *p*-values were adjusted for
23 multiple testing by calculating Storey's *q*-values using *fdrtooltrimmer*. For each gene, the

1 *q*-value is the smallest false discovery rate at which the gene is found significant. We
2 analyzed biological processes as defined by the Gene Ontology Consortium. Each gene
3 ontology term defines a set of genes. The entire list of genes, sorted by the *q*-value in
4 ascending order, is subjected to a non-parametric variant of the Gene Set Enrichment
5 Analysis (GSEA), in which the parametric Kolmogorov-Smirnov *p*-value is replaced with
6 the exact rank-order *p*-value. We perform a Bonferroni adjustment of gene set *p*-values
7 for the number of gene sets tested. Heatmaps of expression levels were created using
8 in-house hierarchical clustering software that implements Ward clustering. The colors
9 qualitatively correspond to fold changes. Complete sequence data can be observed at
10 <http://www.ncbi.nlm.nih.gov/geo/query/acc.cgi?token=yfwtskeirrefbsp&acc=GSE58318>
11 (in vitro macrophage samples)
12 and
13 <http://www.ncbi.nlm.nih.gov/geo/query/acc.cgi?token=kpqnyqalfgnlgd&acc=GSE84535>
14 (in vivo tumor and tumor associated macrophages samples).

15

16 **Individual quantitative RT-PCR**

17 cDNA was prepared using 1µg RNA with the qScript cDNA Synthesis Kit (Quanta
18 Biosciences). Sybr green-based qPCR was performed using human and murine primers
19 to *Arg1*, *Ifng*, *Il10*, *Il12p40*, *Il1b*, *Il6*, *Ccl2*, *Vegfa*, *Gapdh*, *Nos2*, *Tgfb1*, *Tnfa* and murine
20 *H2-Aa*, *H2-Ab1*, *H2-Eb1*, and *H60a* (Qiagen QuantiTect Primer Assay). mRNA levels
21 were normalized to *Gapdh* ($dCt = Ct \text{ gene of interest} - Ct \text{ Gapdh}$) and reported as
22 relative mRNA expression ($ddCt = 2^{-(dCt \text{ sample} - dCt \text{ control})}$) or fold change.

23

1 **siRNA mediated knockdown and gene transfection**

2 Freshly isolated bone marrow derived CD11b⁺ myeloid cells or differentiated
3 macrophages were transfected by electroporation using an AMAXA Mouse Macrophage
4 Nucleofection Kit with 100nM of siRNA or 2µg p110gCAAX or pcDNA control plasmid.
5 Non-silencing (Ctrl_AllStars_1), *Cebpb* (MmCebpb_4 and MmCebpb_6), *Mtor*
6 (Mm_Frap1_1 and Mm_Frap1_2) were purchased from Qiagen. After transfection, cells
7 were cultured for 36-48 h in RPMI containing 10% serum and 10ng/ml M-CSF
8 (PeproTech) or polarized as described above.

9

10 **ELISA assays**

11 Whole tumors, CD11b⁺Gr1⁻ cells, CD90.2⁺ cells, CD4⁺ cells and CD8⁺ cells isolated
12 from LLC tumors were lysed in RIPA buffer and total protein concentration was
13 determined using a BCA Protein Assay (Pierce). Macrophage supernatants (100 µl) or
14 500 µg of total protein lysate from tumors were used in ELISAs to detect CCL2, TGFβ,
15 IL-1β, TNFα, IL-6, IFNγ, IL-10, IL-12 and Granzyme B (Ready Set Go ELISA,
16 eBioscience). Protein expression was normalized to total volume (supernatants) or mg
17 total protein (tumor lysates).

18

19 **Quantitative Colorimetric Arginase Determination**

20 The QuantiChrom Arginase Assay Kit (DARG-200, BioAssay Systems) was used to
21 measure Arginase activity in primary murine bone marrow derived macrophages from
22 wildtype and p110γ^{-/-} mice according to manufacturer's instructions. For all conditions,
23 cells were harvested and lysed in 10 mM Tris (pH7.4) containing 1 µM pepstatin A, 1

1 μ M leupeptin, and 0.4% (w/v) TritonX-100. Samples were centrifuged at 20,000g at 4°C
2 for 10 min.

3

4 **Transcription Factor Assays**

5 To measure NF κ B and C/EBP β activation, TransAM NF κ B Family and C/EBPa/b
6 Transcription Factor Assay Kits (43296 and 44196, Active Motif, Carlsbad, CA) were
7 used according to manufacturer's protocol. Briefly, wild type and p110 γ ^{-/-} bone marrow
8 derived macrophages were stimulated with LPS (100 ng/ml) or IL-4 (20 ng/ml) and
9 nuclear extracts were prepared in lysis buffer AM2. Nuclear extracts were incubated
10 with the immobilized consensus sequences and RelA, cRel or C/EBP β were detected
11 using specific primary antibodies. Quantification was performed via colorimetric readout
12 of absorbance at 450 nm.

13

14 **Immunoblotting**

15 IL-4 and LPS macrophage cultures were solubilized in RIPA buffer containing protease
16 and phosphatase inhibitors. Thirty μ g protein was electrophoresed on Biorad precast
17 gradient gels and electroblotted onto PVDF membranes. Proteins were detected by
18 incubation with 1:1000 dilutions of primary antibodies, washed and incubated with Goat
19 anti-rabbit-HRP antibodies and detected after incubation with a chemiluminescent
20 substrate. Primary antibodies directed against Akt (11E7), p-Akt (244F9), I κ Ba (L35A5),
21 IKKb (D30C6), p-IKKa/b (16A6), NF κ Bp65 (D14E12), pNF κ Bp65 (93H1), C/EBPb
22 (#3087), p-CEBPb (#3082), IRAK1 (D51G7), TBK1 (D1B4), and p110 γ (#4252) were
23 from Cell Signaling Technology and pTBK1 (EPR2867(2)) was from Abcam.

1

2 **In vitro cytotoxicity assay**

3 CD90.2+ tumor derived T cells were purified from LLC tumor-bearing WT and p110 γ ^{-/-}
4 or TG100-115 and control treated mice and then co-incubated with LLC tumor cells
5 (target cells) at 2.5:1, 5:1 and 10:1 ratios of T cells to tumor cells (2x10³ LLC tumor cells
6 per well) for 6 hours. Target cell killing was assayed by collecting the supernatants from
7 each well for measurement of the lactate dehydrogenase release (Cytotox96 Non
8 Radioactive Cytotoxicity Assay kit, Promega).

9

10 **Immunohistochemistry**

11 Tumor samples were collected and cryopreserved in O.C.T. Sections (5 μ m) were fixed
12 in 100% cold acetone, blocked with 8% normal goat serum for 2 hours, and incubated
13 anti-CD8 (53-6.7, 1:50 BD Biosciences) for 2 hours at room temperature. Sections were
14 washed 3 times with PBS and incubated with Alexa594-conjugated secondary
15 antibodies. Slides were counterstained with 4',6-diamidino-2-phenylindole (DAPI) to
16 identify nuclei. Immunofluorescence images were collected on a Nikon microscope
17 (Eclipse TE2000-U) and analyzed using Metamorph image capture and analysis
18 software (Version 6.3r5, Molecular Devices). The detection of apoptotic cells was
19 performed using a TUNEL-assay (ApopTag Fluorescein In Situ Apoptosis Detection Kit,
20 Promega) according to manufacturer's instructions. Slides were washed and mounted in
21 DAKO fluorescent mounting medium. Immunofluorescence images were collected on a
22 Nikon microscope (Eclipse TE2000-U) and analyzed with MetaMorph Software (version

1 6.3r5) or SPOT software (version 4.6). Pixels/field or cell number/field were quantified in
2 five 100x fields from 10 biological replicates.

3

4 **Statistics**

5 Primary tumor samples with mRNA expression data were scored as above or below the
6 median expression level, and tested for association with patient survival using a logrank
7 test at 5% significance. For studies evaluating the effect of drugs on tumor size, tumor
8 dimensions were measured directly before the start of treatment, tumor volumes were
9 computed and mice were randomly assigned to groups so that the mean volume +/-
10 s.e.m. of each group was identical. A sample size of 10 mice/group provided 80%
11 power to detect mean difference of 2.25 standard deviation (SD) between two groups
12 (based on a two-sample t-test with 2-sided 5% significance level). Sample sizes of 15
13 mice/group provided 80% power to detect one SD difference between two groups. Data
14 were normalized to the standard (control). Significance testing was performed by one-
15 way Anova with Tukey's posthoc testing for multiple pairwise testing with more than two
16 groups and by parametric or nonparametric Student's *t* test when only two groups were
17 compared. We used a two-sample t-test (two groups) and ANOVA (multiple groups)
18 when data were normally distributed and a Wilcoxon rank sum test (two groups) when
19 data were not normally distributed. All mouse studies were randomized and blinded;
20 assignment of mice to treatment groups, tumor measurement and tumor analysis was
21 performed by coding mice with randomly assigned mouse number, with the key
22 unknown to operators until experiments were completed. In tumor studies for which
23 tumor size was the outcome, animals removed from the study due to health concerns

- 1 were not included in endpoint analyses. All experiments were performed at least twice;
- 2 n refers to biological replicates.

1 **References**

- 2 1 Sica, A. & Mantovani, A. Macrophage plasticity and polarization: in vivo veritas. *J*
3 *Clin Invest* **122**, 787-795 (2012).
- 4 2 Schmid, M. C. & Varner, J. A. Myeloid cells in tumor inflammation. *Vasc Cell* **4**,
5 14, (2012).
- 6 3 Wynn, T. A., Chawla, A. & Pollard, J. W. Macrophage biology in development,
7 homeostasis and disease. *Nature* **496**, 445-455 (2013).
- 8 4 Tabas, I. & Glass, C. K. Anti-inflammatory therapy in chronic disease: challenges
9 and opportunities. *Science* **339**, 166-172 (2013).
- 10 5 Ruffell, B. & Coussens, L. M. Macrophages and therapeutic resistance in cancer.
11 *Cancer Cell* **27**, 462-472 (2015).
- 12 6. Sharma, P. & Allison, J. P. The future of immune checkpoint therapy. *Science*
13 **348**, 56-61 (2015).
- 14 7. Topalian, S. L., Drake, C. G. & Pardoll, D. M. Immune checkpoint blockade: a
15 common denominator approach to cancer therapy. *Cancer Cell* **27**, 450-461 (2015).
- 16 8. <https://gdc-portal.nci.nih.gov/projects/TCGA-HNSC> (accessed 12/23/2015) and
17 <https://gdc-portal.nci.nih.gov/projects/TCGA-LUAD> (accessed 3/14/2016).
- 18 9. Martini, M., De Santis, M. C., Braccini, L., Gulluni, F. & Hirsch, E. PI3K/AKT
19 signaling pathway and cancer: an updated review. *Ann Med* **46**, 372-383 (2014).
- 20 10. Vanhaesebroeck, B., Stephens, L. & Hawkins, P. PI3K signalling: the path to
21 discovery and understanding. *Nat Rev Mol Cell Biol* **13**, 195-203 (2012).
- 22 11. Martin, E. L. et al. Phosphoinositide-3 kinase gamma activity contributes to sepsis
23 and organ damage by altering neutrophil recruitment. *Am J Respir Crit Care Med* **182**,

- 1 762-773 (2010).
- 2 12. Schmid, M. C. et al. Receptor tyrosine kinases and TLR/IL1Rs unexpectedly
3 activate myeloid cell PI3kgamma, a single convergent point promoting tumor
4 inflammation and progression. *Cancer Cell* **19**, 715-727 (2011).
- 5 13. Gunderson, A. J., Kaneda, M.M. et al. Bruton Tyrosine Kinase-Dependent
6 Immune Cell Cross-talk Drives Pancreas Cancer. *Cancer Discov.* **6**, 270-285
7 (2015).
- 8 14. Schmid, M. C. et al. PI3-kinase gamma promotes Rap1a-mediated activation of
9 myeloid cell integrin alpha4beta1, leading to tumor inflammation and growth. *PLoS One*
10 **8**, e60226 (2013).
- 11 15. Kaneda, M.M, et al. Macrophage PI3Ky drives pancreatic ductal adenocarcinoma
12 progression. *Cancer Discov.* **6**, 870-875 (2016).
- 13 16. Evans, C.A., et al. Discovery of a Selective Phosphoinositide-3-Kinase (PI3K)
14 (PI3K) γ Inhibitor (IPI-549) as an Immuno-Oncology Clinical Candidate. *ACS Med.*
15 *Chem. Lett.* in press (2016). 10.1021/acsmedchemlett.6b00238.
- 16 17. Ben-Neriah, Y. & Karin, M. Inflammation meets cancer, with NF-kappaB as the
17 matchmaker. *Nat Immunol* **12**, 715-723 (2011).
- 18 18. Poli, V. The role of C/EBP isoforms in the control of inflammatory and native
19 immunity functions. *J Biol Chem* **273**, 29279-29282 (1998).
- 20 19. Gray, M. J., Poljakovic, M., Kepka-Lenhart, D. & Morris, S. M., Jr. Induction of
21 arginase I transcription by IL-4 requires a composite DNA response element for STAT6
22 and C/EBPbeta. *Gene* **353**, 98-106 (2005).
- 23 20. van Rooijen N, Kors N, ter Hart H, Claassen E. In vitro and in vivo elimination of

1 macrophage tumor cells using liposome-encapsulated dichloromethylene
2 diphosphonate. *Virchows Arch B Cell Pathol Incl Mol Pathol.* **54**, 241-245 (1988).

3 21. Pyonteck, S. M. et al. CSF-1R inhibition alters macrophage polarization and
4 blocks glioma progression. *Nat Med* **19**, 1264-1272 (2013).

5 22. Chaurasia, B. et al. Phosphoinositide-dependent kinase 1 provides negative
6 feedback inhibition to Toll-like receptor-mediated NF-kappaB activation in
7 macrophages. *Mol Cell Biol* **30**, 4354-4366 (2010).

8 23. Arranz, A. et al. Akt1 and Akt2 protein kinases differentially contribute to
9 macrophage polarization. *Proc Natl Acad Sci U S A* **109**, 9517-9522 (2012).

10 24. Byles, V. et al. The TSC-mTOR pathway regulates macrophage polarization. *Nat*
11 *Commun* **4**, 2834 (2013).

12 25. Yue, S. et al. Myeloid PTEN deficiency protects livers from ischemia reperfusion
13 injury by facilitating M2 macrophage differentiation. *J Immunol* **192**, 5343-5353 (2014).

14 26. Rauh, M.J., et al. SHIP represses the generation of alternatively activated
15 macrophages. *Immunity* **23**, 361-374 (2005).

16 27. Baer C, et al. Suppression of microRNA activity amplifies IFN- γ -induced
17 macrophage activation and promotes anti-tumour immunity. *Nat Cell Biol.* **18**, 790-802
18 (2016).

19 28. Gyorffy, B., Surowiak, P., Budczies, J. & Lanczky, A. Online survival analysis
20 software to assess the prognostic value of biomarkers using transcriptomic data in non-
21 small-cell lung cancer. *PLoS One* **8**, e82241(2013).

1 **Extended Data Figure 1: Pro-inflammatory gene expression signatures predict**
2 **survival in cancer patients**

3 (a-e) Expression levels of *IL12A*, *IL12B*, *IFNG*, and *CD8A*, and *IL6* associated with
4 survival in HPV+ HNSCC patients. (f) Multivariate immune signature for 720 lung
5 adenocarcinoma patients from KM plotter cohorts. (g) Multivariate immune signature in
6 876 gastric cancer samples from KM plotter cohorts. (h) Western blotting to detect
7 $PI3K\gamma$ (p110 γ) in B cells, T cells, macrophages ($M\Phi$) and LLC, PyMT and MEER tumor
8 cells. (i) Kaplan Meier survival plot of WT and p110 γ ^{-/-} mice inoculated with LPS
9 (endotoxin). (j) Pro-inflammatory cytokine mRNA expression in bone marrow from WT
10 and p110 γ ^{-/-} LPS injected animals (n=4, ***p*<0.001, ****p*<0.0001). (k) Circulating
11 inflammatory cytokine levels in p110 γ ^{-/-} and WT mice 24h after endotoxin administration
12 (n=4, **p*<0.01, ***p*<0.001). (l) Tumor volume of HPV- (SCCVII) head and neck (n=15)
13 carcinomas from vehicle or $PI3K\gamma$ inhibitor-treated mice. Arrow, start of drug treatment.
14 (m) Dose response of the effect of $PI3K\gamma$ inhibitor IPI549 on in vitro MEER cell viability.
15 (n) Spontaneous PyMT lung metastases per high power field (200X) in WT and p110 γ ^{-/-}
16 animals (n=8). (o) Kaplan Meier survival plot of mice bearing orthotopic PyMT tumors
17 treated with vehicle or $PI3K\gamma$ inhibitor IPI549 initiated as indicated by arrow (n=10). (p)
18 In vitro LLC tumor cell survival in the presence of gemcitabine. (q) Volume of LLC
19 tumors implanted in WT and p110 γ ^{-/-} animals treated with saline or gemcitabine (n=10,
20 ***p*<0.001, ***p*<0.01).

21

22

1 **Extended Data Figure 2: Effect of PI3K γ inhibition on tumor inflammation**

2 (a) Gating strategy for flow cytometric analysis of myeloid cell populations in peripheral
3 blood leukocytes. (b) Representative flow cytometric analysis and quantification of
4 myeloid cell populations in peripheral blood (PB) of naïve and LLC tumor bearing mice
5 (n = 3). (c) Flow cytometric analysis of myeloid cell populations on days 0, 7, 14 and 21
6 after subcutaneous inoculation with Lewis lung carcinoma cells (n= 3). (d) Quantification
7 of populations from c. (e) Flow cytometric analysis of Ly6G, CCR2, CX3CR1, CD206,
8 CD11c, F4/80 and CD45 expression on myeloid cell populations from c (n=3). (f)
9 Relative immune response transcript levels in tumor-derived myeloid cells and tumor
10 cells (CD11b-Gr1- cells) isolated at day 0 (n=3), d7 (n=5), d14 (n=3) or d21 (n=4) after
11 LLC cell inoculation ($p < 0.002$, $d21$ vs $d0$). (g) Flow cytometric analysis of CD11b+
12 myeloid cell populations in WT and p110 γ -/- LLC, PyMT and MEER tumors (n=3). (h)
13 Quantification of CD11b+ myeloid cell populations from (g). (i) Flow cytometric analysis
14 of CD11b+ myeloid cell populations in vehicle and PI3K γ inhibitor treated PyMT, MEER
15 and SCCVII tumors (n=3). (j). Quantification of CD11b+ myeloid cell populations from
16 (i).
17

1 **Extended Data Figure 3: Effect of PI3K γ inhibition on TAM expression profile**

2 (a) Heatmap of differentially expressed immune response genes in TAMs isolated from
3 LLC tumors from WT and $p110\gamma^{-/-}$ mice (n=3, $*p<0.01$, $lfr <0.1$) obtained by RNA
4 sequencing. (b) Relative mRNA expression of immune response factors in HPV+
5 HNSCC MEER tumors from $p110\gamma^{-/-}$ and WT mice (n=4), $*p=0.01$. (c) Relative mRNA
6 expression of immune response factors in CD11b+ myeloid cells isolated from PyMT
7 tumors grown in vehicle or PI3K γ inhibitor-treated mice (n=4), $*p=0.01$. (d) Fold change
8 in mRNA expression in CD11b+Gr1- (macrophage), CD11b+Gr1lo (monocytic) and
9 CD11b+Gr1hi (granulocytic) myeloid cells isolated from LLC tumors grown in $p110\gamma^{-/-}$
10 mice (n=5) and normalized to WT control (n=5), $p=0.001$. (e) Arginase activity in tumors
11 and TAMs isolated from LLC tumors grown in WT and $p110\gamma^{-/-}$ mice (n=4, $***p<0.0003$).
12 (f) Protein expression of cytokines in LLC tumors and TAMs from WT and $p110\gamma^{-/-}$ mice
13 (n=4, $*p<0.01$, $**p<0.001$, $***p<0.0001$).

14

15

1 **Extended Data Figure 4: Effect of PI3K γ deletion on in vitro macrophage mRNA**
2 **expression**

3 (a) Relative immune response mRNA expression in p110 γ ^{-/-} and WT murine
4 macrophages stimulated by IL-4 or LLC tumor cell conditioned medium (TCM) as
5 determined by RT-PCR (n=3, **p*=0.01). (b) Heat map of differentially expressed immune
6 response transcripts in IL-4 and IFN γ /LPS polarized murine macrophages obtained by
7 RNA sequencing (n=3, *p*=0.00001). (c) Heat map of select differentially expressed
8 immune response transcripts in in vitro polarized murine macrophages (n=3,
9 *p*=0.00001). (d) Heat map of immune response transcripts in mCSF, IL-4 and IFN γ /LPS
10 stimulated p110 γ ^{-/-} murine macrophages obtained by RNA sequencing and normalized
11 to WT (n=3, *p*=0.00001). (e) Heat map of select differentially expressed immune
12 response transcripts in polarized p110 γ ^{-/-} murine macrophages normalized to WT (n=3,
13 *p*=0.00001). (f) Heat map of differentially expressed antigen presentation and
14 processing mRNAs in mCSF, IL-4 and IFN γ /LPS polarized p110 γ ^{-/-} murine
15 macrophages (n=3). (g) Heat map of differentially expressed chemokine and chemokine
16 receptor mRNAs in polarized p110 γ ^{-/-} murine macrophages (n=3).

1 **Extended Data Figure 5: Effect of PI3K γ inhibition on murine and human**
2 **macrophage polarization**

3 (a) Relative mRNA expression of immune response transcripts in IL-4 and IFN γ /LPS
4 stimulated vehicle and PI3K γ inhibitor (IPI-549) treated (a) murine and (b) human
5 macrophages (n=3, $p=0.001$). (c) Relative mRNA expression of M2 macrophage
6 markers (*Arg1*, *Fizz1* and *Ym1*) in WT and *p110 γ ^{-/-}* IL4-stimulated macrophages (n=3).
7 (d) Relative expression of MHC family members in WT and *p110 γ ^{-/-}* IL4-stimulated
8 macrophages (n=3). (e-f) Time course of cytokine mRNA expression in IFN γ /LPS, LPS
9 and IL-4 stimulated (e) WT vs *p110 γ ^{-/-}* and (f) vehicle vs. PI3K γ inhibitor (IPI-549)-
10 treated macrophages (n=3). (g) Relative mRNA expression in mCSF-stimulated WT vs
11 *p110 γ ^{-/-}* and IPI-549- vs vehicle-treated macrophages (n=3). (g) Relative nuclear RelA
12 DNA binding activity in IFN γ /LPS stimulated WT and *p110 γ ^{-/-}* macrophages (n=3).

1 **Extended Data Figure 6: Mechanism of PI3K γ mediated gene expression**
2 **regulation**

3 (a) Relative levels of phospho/total p65 and phospho/total C/EBP β in LPS and IL-4
4 stimulated WT and p110 γ ^{-/-} macrophages. (b) Immunoblotting to detect pThr308Akt,
5 total Akt, phospho-p65 and total p65 in LPS and IL-4 stimulated, macrophages that
6 were treated with vehicle or the PI3K γ inhibitor IPI-549. (c) Relative *Arg1* mRNA
7 expression in myeloid cells transfected with constitutively active, membrane-targeted
8 PI3K γ (*p110 γ CAAX*) and *Mtor*, *S6ka*, *Cebpb* or control siRNA (n=3). (d) Validation of
9 siRNAs from c. (e) Effect of *Cebpb*, *Mtor* or *S6ka* siRNAs on gene expression in WT
10 macrophages. (f-g) Effect of rapamycin (f) or S6K inhibitor (PF4708671) (g) on
11 macrophage mRNA expression. (h) Immunofluorescence images of CD8⁺ T cells in
12 10 μ m tumor sections from 3c. (i) Mean tumor volumes from tumor cells mixed with WT
13 TAMs pretreated with the mTOR inhibitor Rapamycin or the Arginase inhibitor nor-
14 NOHA and p110 γ ^{-/-} TAMs pretreated with anti-IL12 or isotype matched control antibody
15 (cIgG), IKK β inhibitor (MLB120) or NOS2 inhibitor (1400W dihydrochloride) (n=10).

1 **Extended Data Figure 7: No direct effect of PI3K γ inhibition on T cells**

2 (a) Volumes of LLC tumors treated with vehicle + control liposomes, PI3K γ inhibitor (IPI-
3 549) + control liposomes, clodronate liposomes + vehicle and PI3K γ inhibitor +
4 clodronate liposomes (n=10). (b) Quantification of F4/80+ macrophages in tumors from
5 a (n=3). (c) Quantification of F4/80+ macrophages in livers from a (n=3). (d)
6 Quantification of T cells in tumors from a (n=3, *p<0.05). (e) Volumes of CT26 tumors
7 treated with vehicle + clgG, PI3K γ inhibitor (IPI-549) + clgG, anti-CD115 + vehicle and
8 PI3K γ inhibitor + anti-CD115 (n=15). (f) Quantification of CD11b+ myeloid cells in
9 tumors from e (n=5). (g) Images and quantification of CD8+ T cells in WT and p110 γ ^{-/-}
10 LLC tumors by IHC (n=5). (h) Flow cytometric analysis and quantification of T cell
11 populations in tumors from WT and p110 γ ^{-/-} or IPI-549 treated animals (n=3). (i)
12 Quantification of T cells in spleens of naïve and LLC tumor-bearing WT and p110 γ ^{-/-}
13 mice (n=3). (j) Volumes of LLC lung tumors from WT, p110 γ ^{-/-}, CD8^{-/-} and CD8^{-/-}; p110 γ ^{-/-}
14 animals (n=12). (k) LLC tumor volume from WT and p110 γ ^{-/-} animals treated with anti-
15 CD8 antibodies or control (n=10) and percent CD8+ T cells in these tumors (n=3). (l) In
16 vitro proliferation of T cells isolated from naïve and LLC tumor-bearing WT and p110 γ ^{-/-}
17 mice (n=3). (m) IFN γ and Granzyme B protein expression in T cells from l (n=3).

1 **Extended Data Figure 8: PI3K γ inhibition relieves T cell exhaustion**

2 (a) Effect of PI3K γ and PI3K δ inhibitors on IFN γ expression by activated human T cells
3 (n=3). (b) Mean weights of tumors derived from a mixture of LLC cells and WT or p110 γ -
4 /- tumor derived T cells or WT T cells pre-incubated with 10 or 100 nM PI3K γ (IPI-549)
5 and PI3K δ (Cal101) inhibitors prior to implantation (n=16). (c-d) In vitro LLC tumor cell
6 cytotoxicity induced by T cells isolated from LLC tumors from (c) WT and p110 γ -/- or (d)
7 control- and PI3K γ inhibitor-treated mice (n=3, * $p < 0.001$). (e) Images of TUNEL and
8 H&E stained tumors as described in Fig. 5c. (f) Quantification of TUNEL+ cells in tumor
9 sections from e. (g) Mean tumor volumes in WT mice derived from LLC tumor cells
10 mixed 1:1 with CD90.2+, CD4+ and CD8+ T cells or no T cells from WT or p110 γ -/-
11 tumor-bearing animals (n=8). (h) IL10 and TGF β protein expression in lysates from
12 tumor and CD90.2+, CD8+ and CD4+ T cells isolated from LLC tumors grown in WT
13 and p110 γ -/- animals (n=3). (i) Interferon gamma and Granzyme B protein expression in
14 PI3K γ inhibitor or control-treated LLC tumors (n=3). (j) *Ifn γ* and *Tgfb1* mRNA expression
15 in T cells isolated from LLC tumors grown in WT and p110 γ -/- or control- and PI3K γ
16 inhibitor-treated mice (n=3). (k) Relative mRNA expression of *Cd4*, *Cd8*, *Grzb* and *Ifng*
17 in control and PI3K γ inhibitor treated PyMT tumors (n=3). (l) Relative mRNA expression
18 of *Cd4*, *Cd8*, *Grzb*, and *Ifng* in WT and p110 γ -/- and PI3K γ inhibitor treated HPV+ MEER
19 tumors (n=3).

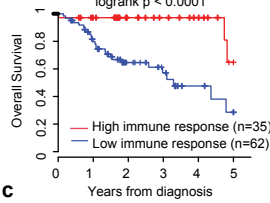
1 **Extended Data Figure 9: PI3K γ role in the macrophage-mediated tumor immune**
2 **response**

3 (a-b) Flow cytometric analysis of PD-L1 and PD-L2 expression on (a) tumor cells and
4 TAMs from WT and p110 γ ^{-/-} LLC tumors and (b) WT and p110 γ ^{-/-} in vitro cultured
5 IFN γ /LPS- and IL4-stimulated macrophages (n=3). (c) HPV+ HNSCC tumor growth in
6 female WT or p110 γ ^{-/-} mice that were treated with anti-PD-1 or isotype matched
7 antibody (clgG), as indicated by arrows, and percent change in tumor volumes between
8 days 11 and 23. (d) HPV+ HNSCC tumor growth in female WT mice that were treated
9 with PI3K γ inhibitor (2.5 mg/kg TG100-115 b.i.d). in combination with anti-PD-1 or
10 isotype matched antibody (clgG), as indicated by arrows, and percent change in tumor
11 volumes 11 and 29. (e) HPV- HNSCC tumor growth in mice that were treated with PI3K γ
12 inhibitor (2.5 mg/kg TG100-115 b.i.d) in combination with anti-PD-1 clgG, as indicated
13 by arrows, and percent change in tumor volumes between days 19-26. (f) Tumor
14 rechallenge in HPV+ mice that had cleared previously HPV+ tumors (n=7-12) vs WT
15 mice (n=5). (g) Quantification of percent CD3, CD4+ and CD8+ T cells and MHCII+
16 macrophages from Figure 5l. (* p <0.05, ** p <0.005, **** p <0.00005).

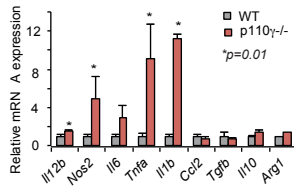
1 **Extended Data Figure 10: PI3K γ promotes immune suppression.**

2 (a) Comparison of gene expression between HPV+ and HPV- cohorts indicating HPV-
3 samples had significantly ($p < 0.05$) lower expression of adaptive immune genes and
4 higher expression of immune suppressive/pro-metastasis genes (Blue: HPV- samples,
5 Red: HPV+ samples.) (b) Model depicting the effect of PI3K γ inhibition on tumor
6 immune suppression. PI3K γ inhibition converts tumor-associated macrophages into pro-
7 inflammatory macrophages that promote a CD8+ T cell response that suppresses tumor
8 growth. (c) Model depicting the PI3K γ signaling pathway in macrophages. PI3K γ
9 activation restrains NF κ B activation and promotes mTOR-dependent C/EBP β activation,
10 leading to expression of immune suppressive factors and tumor growth. In contrast,
11 PI3K γ inhibition inhibits C/EBP β and stimulates NF κ B, leading to altered expression of
12 pro-inflammatory immune response cytokines.

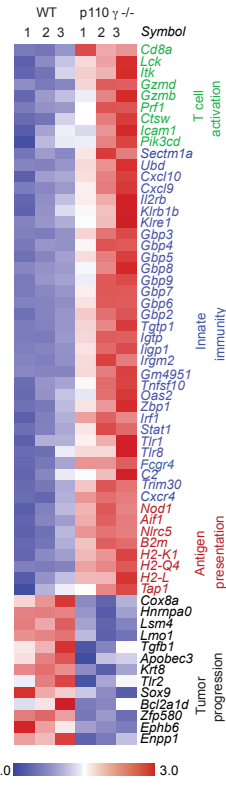
a HPV+ Immune Multi-Gene Signature



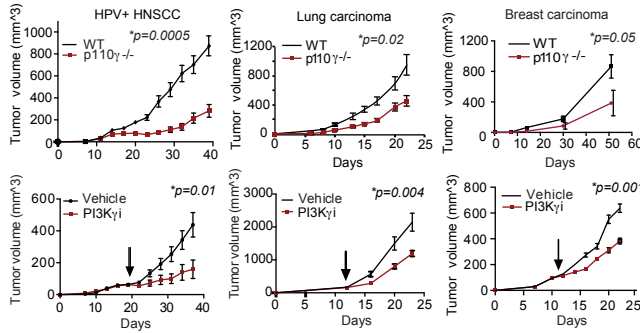
b



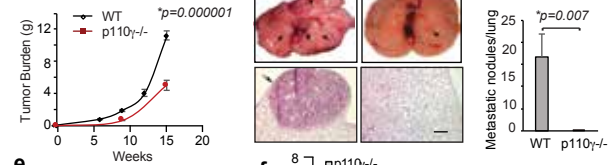
g



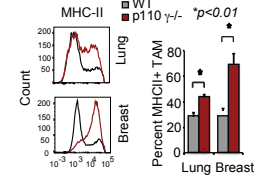
c



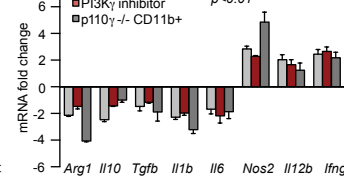
d Spontaneous breast carcinoma

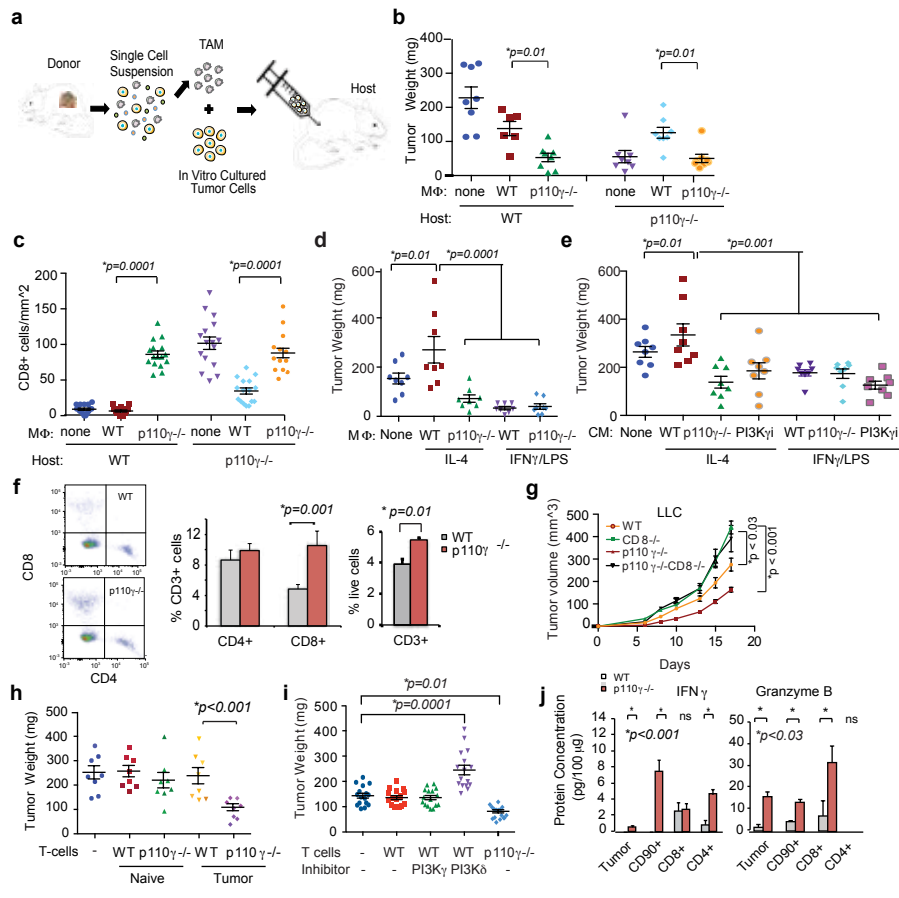


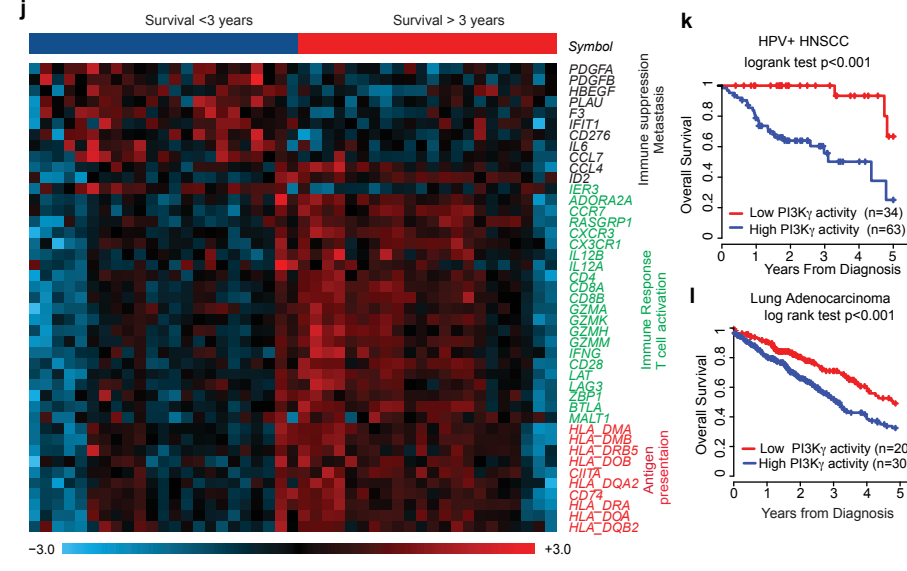
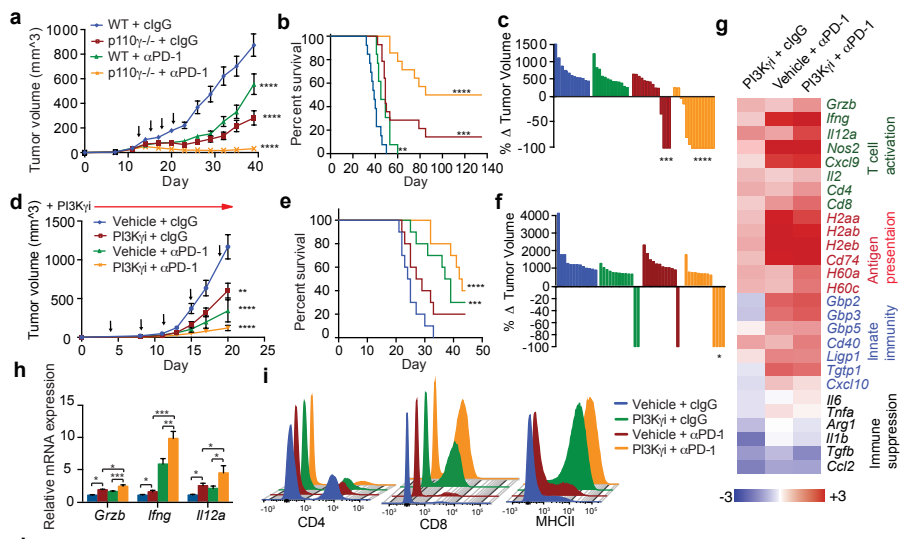
e

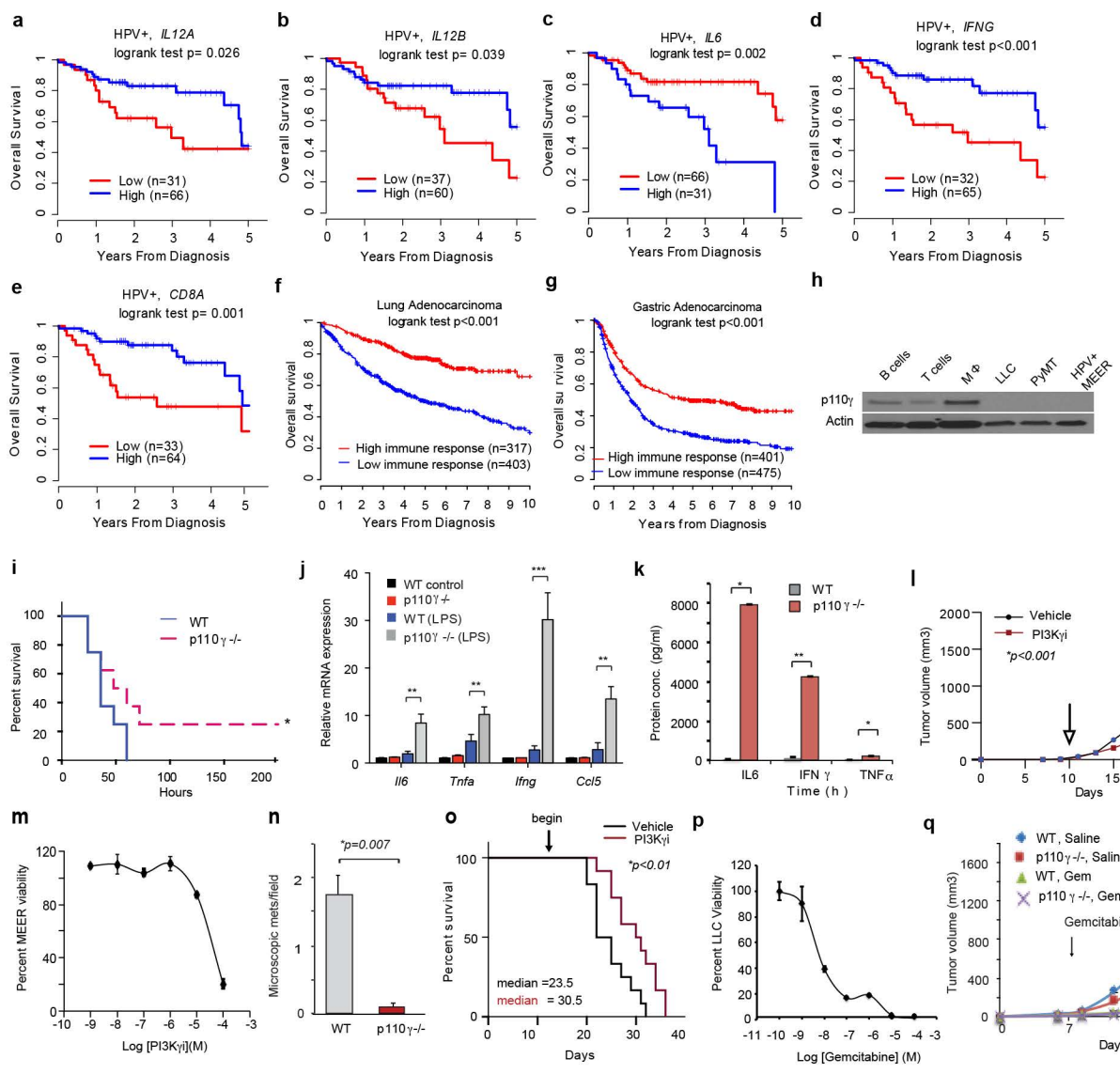


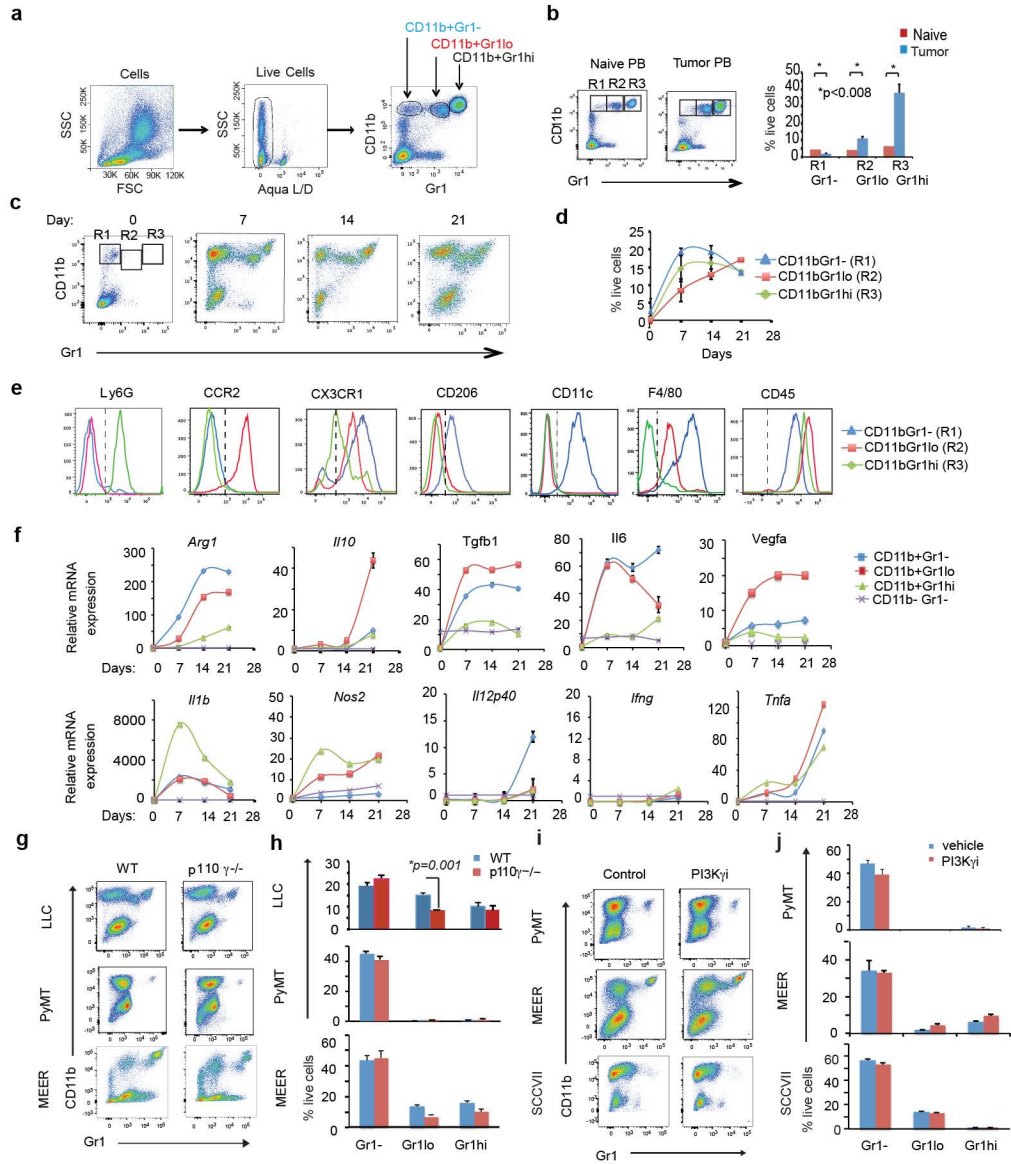
f

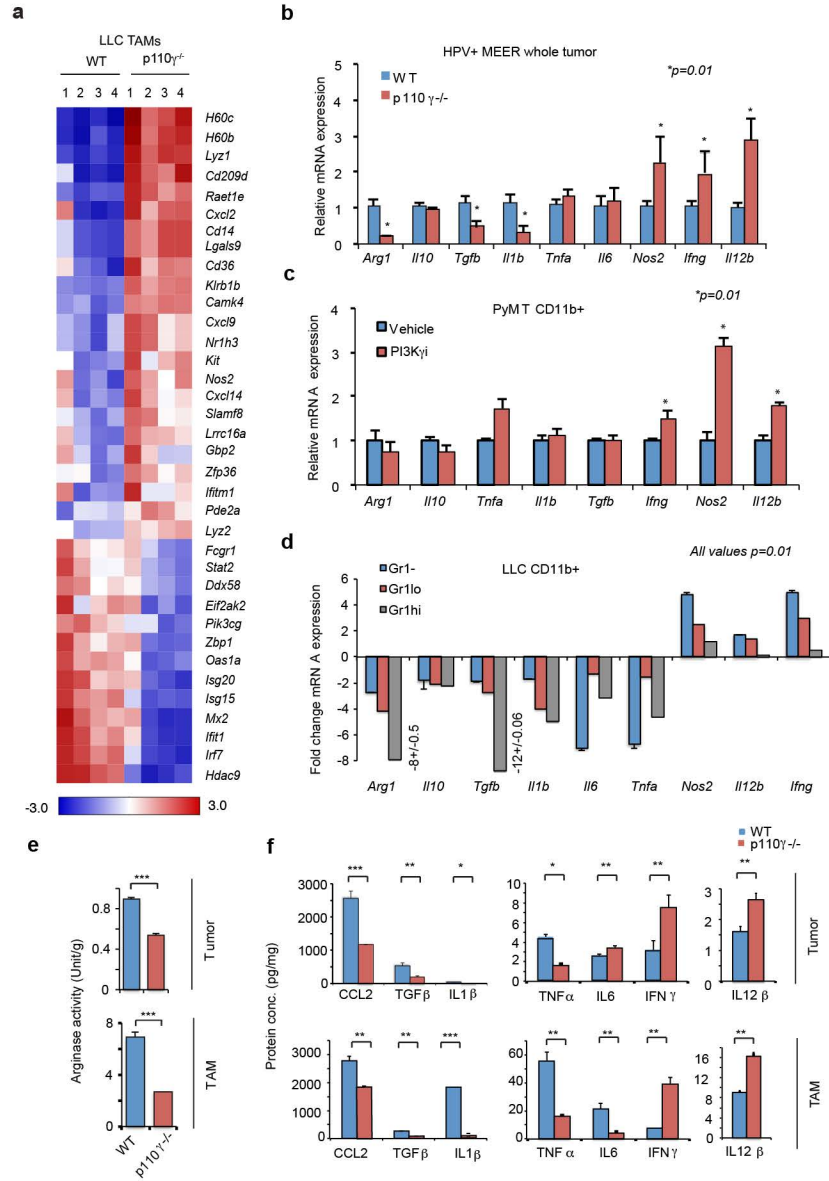


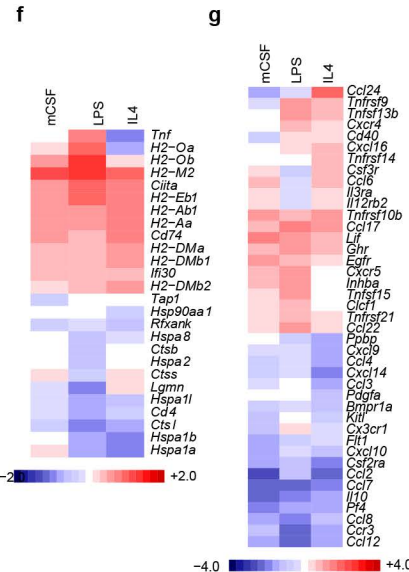
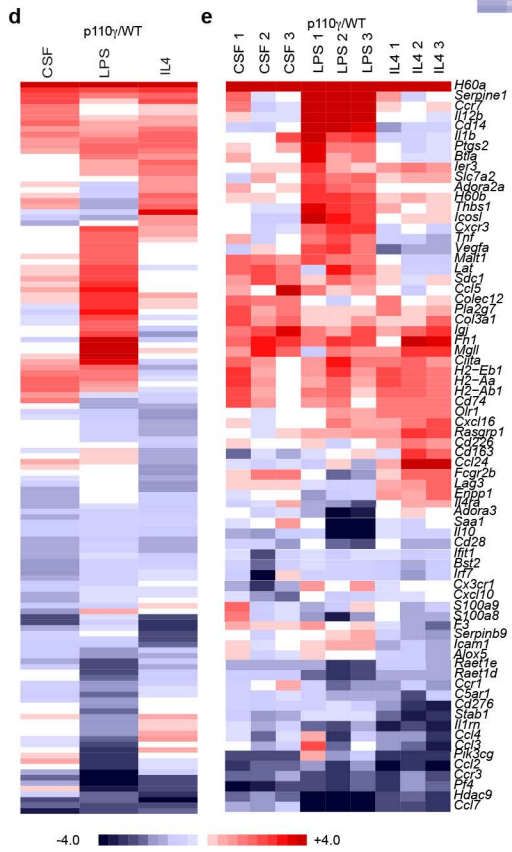
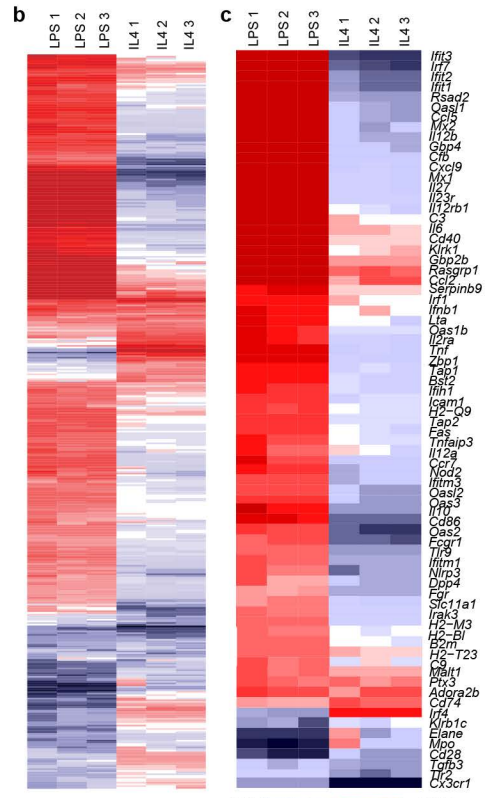
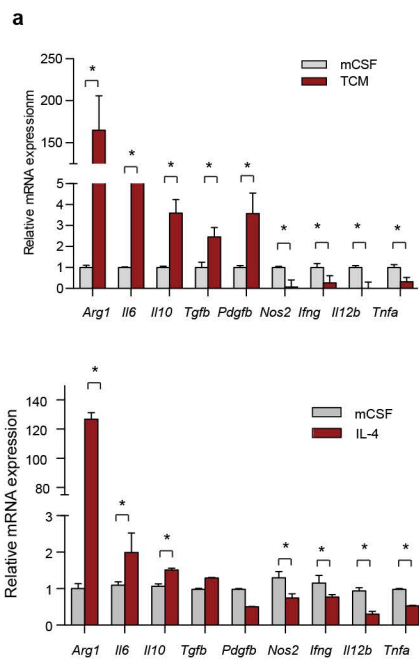


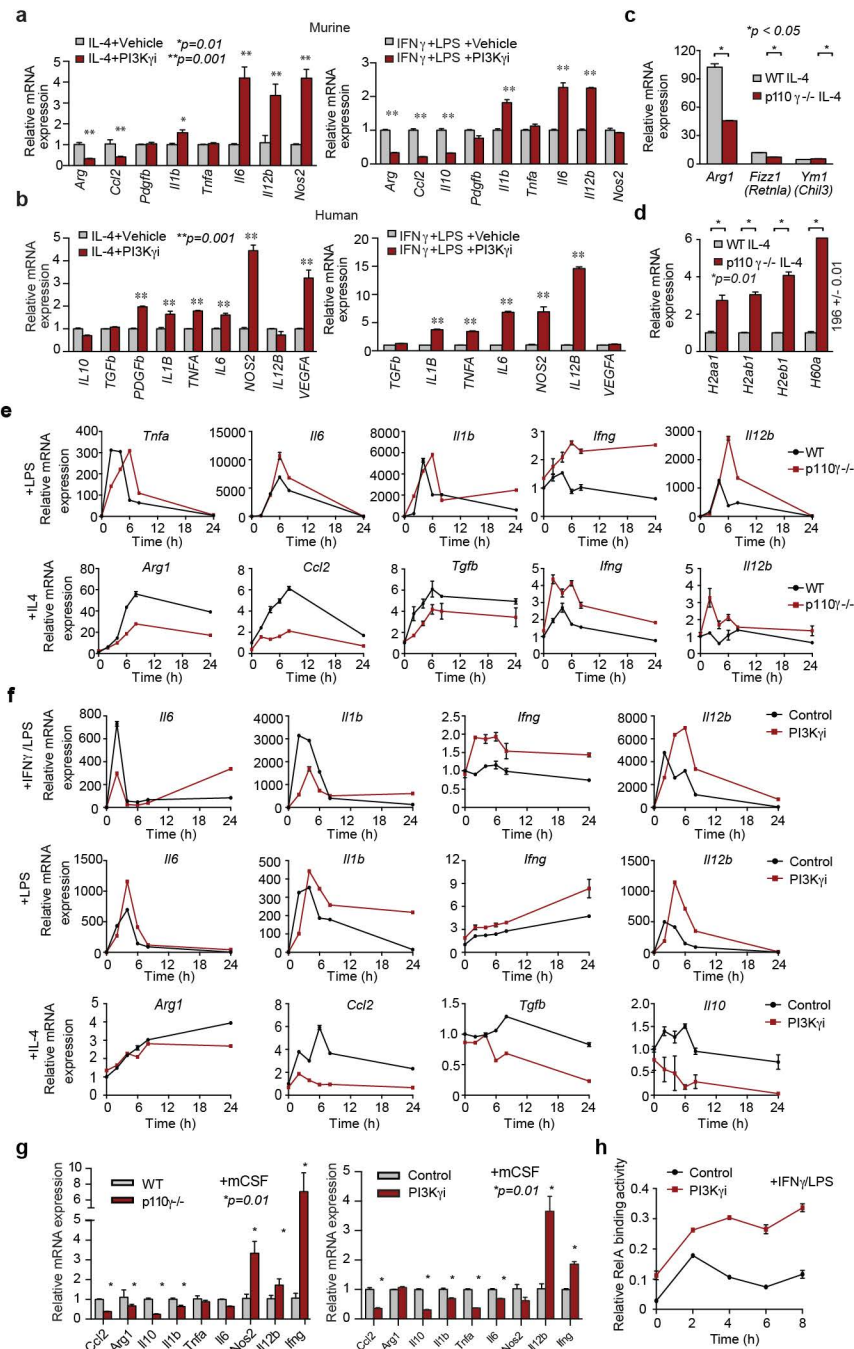


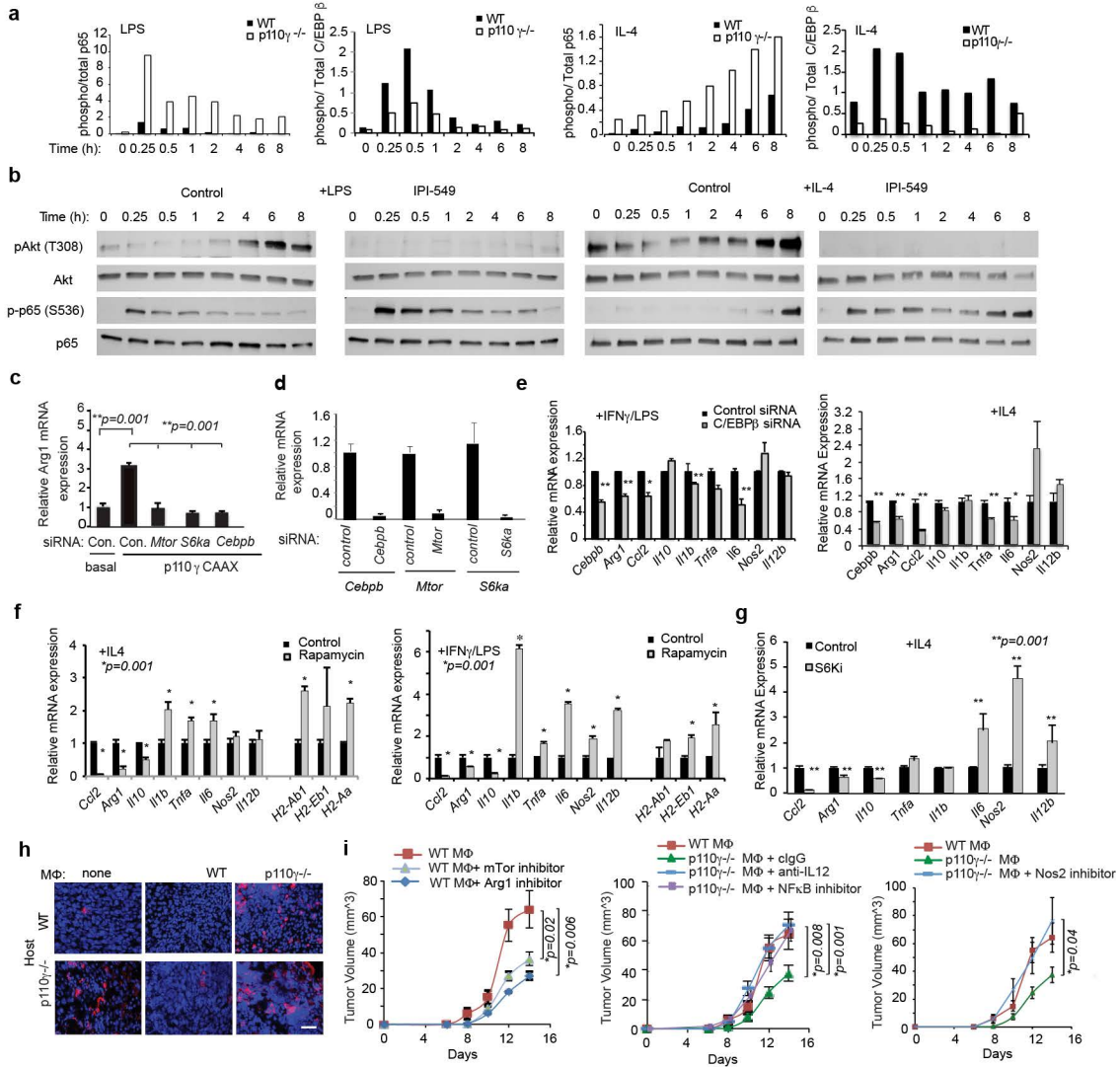


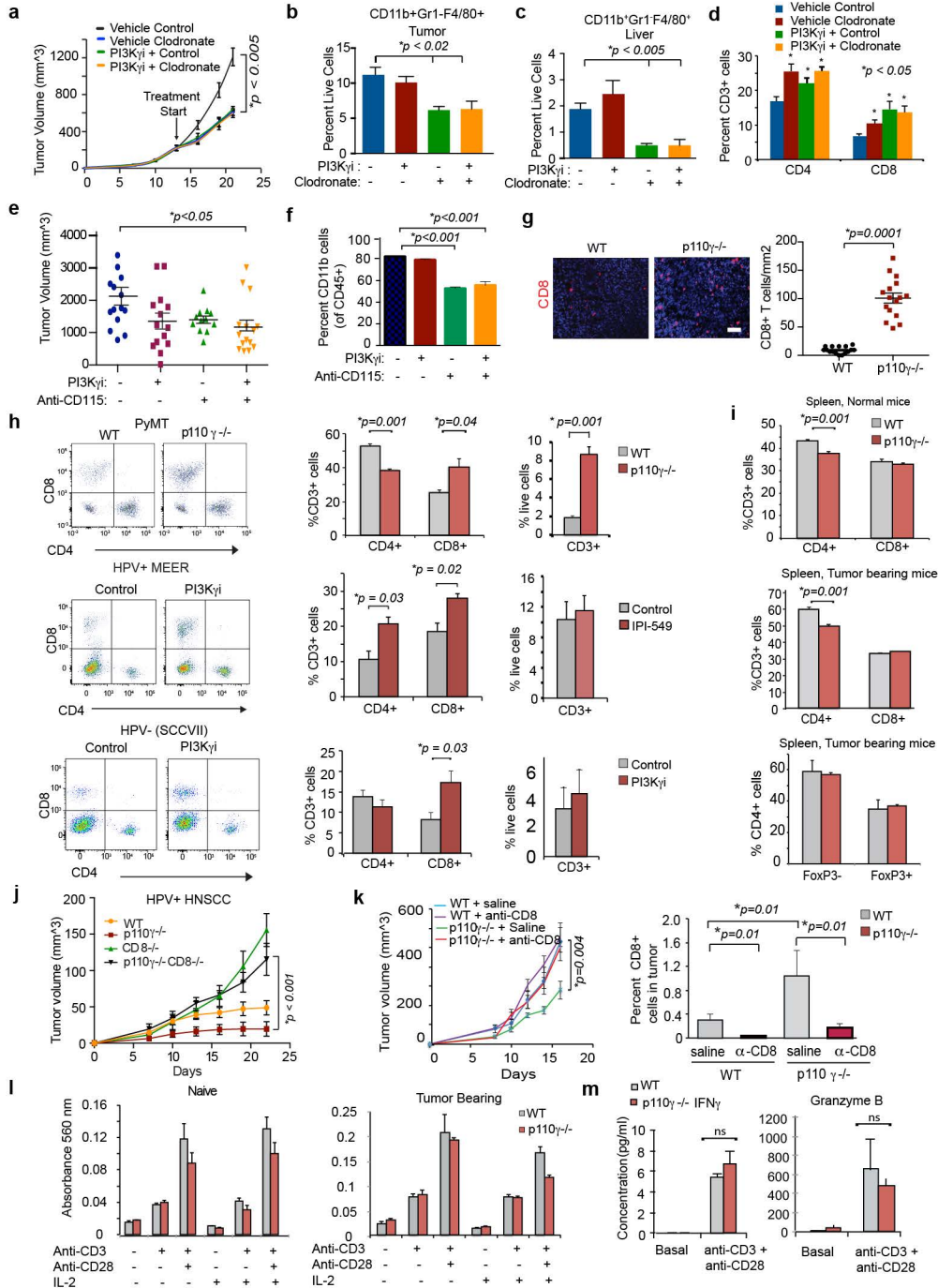


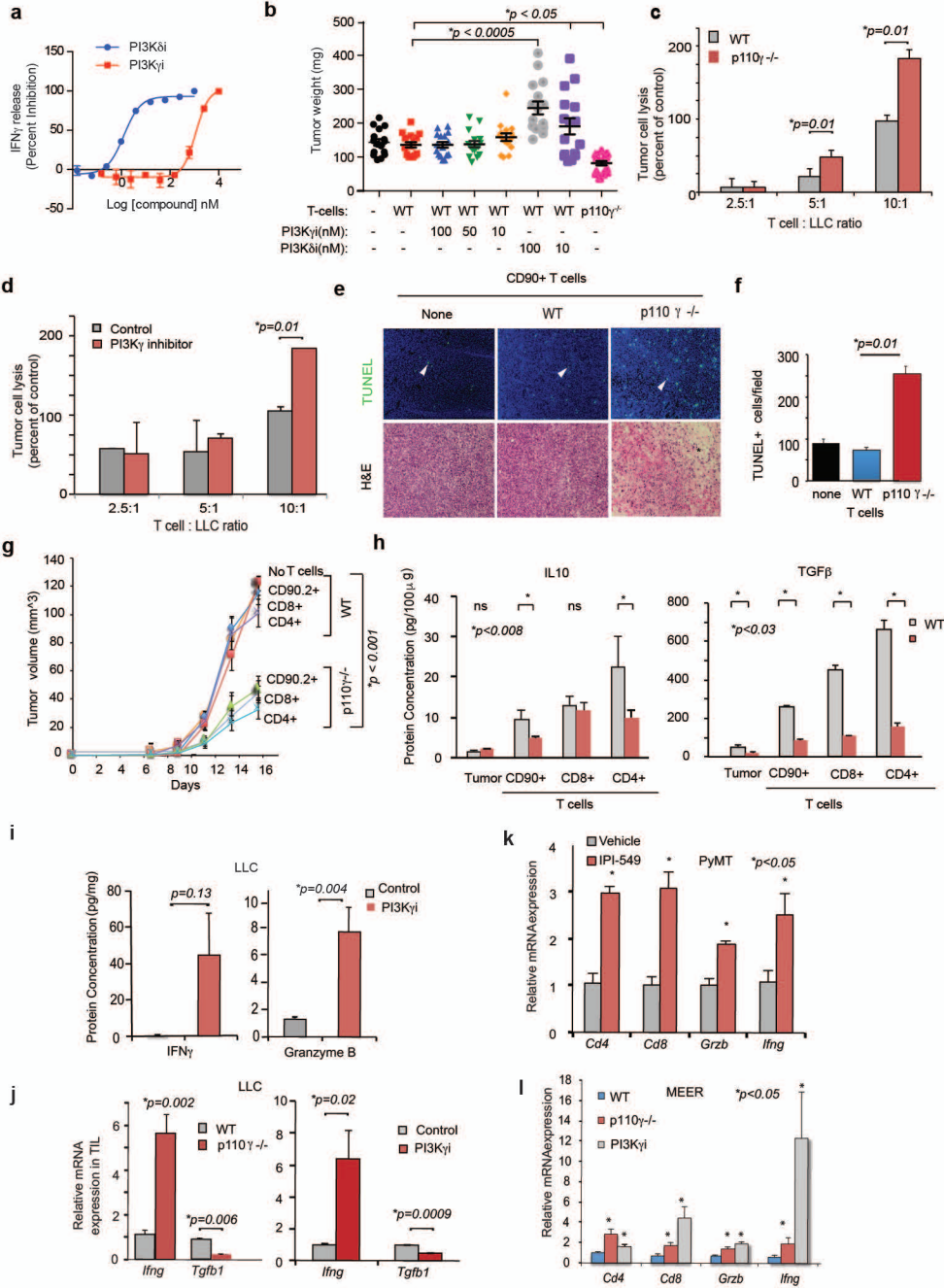


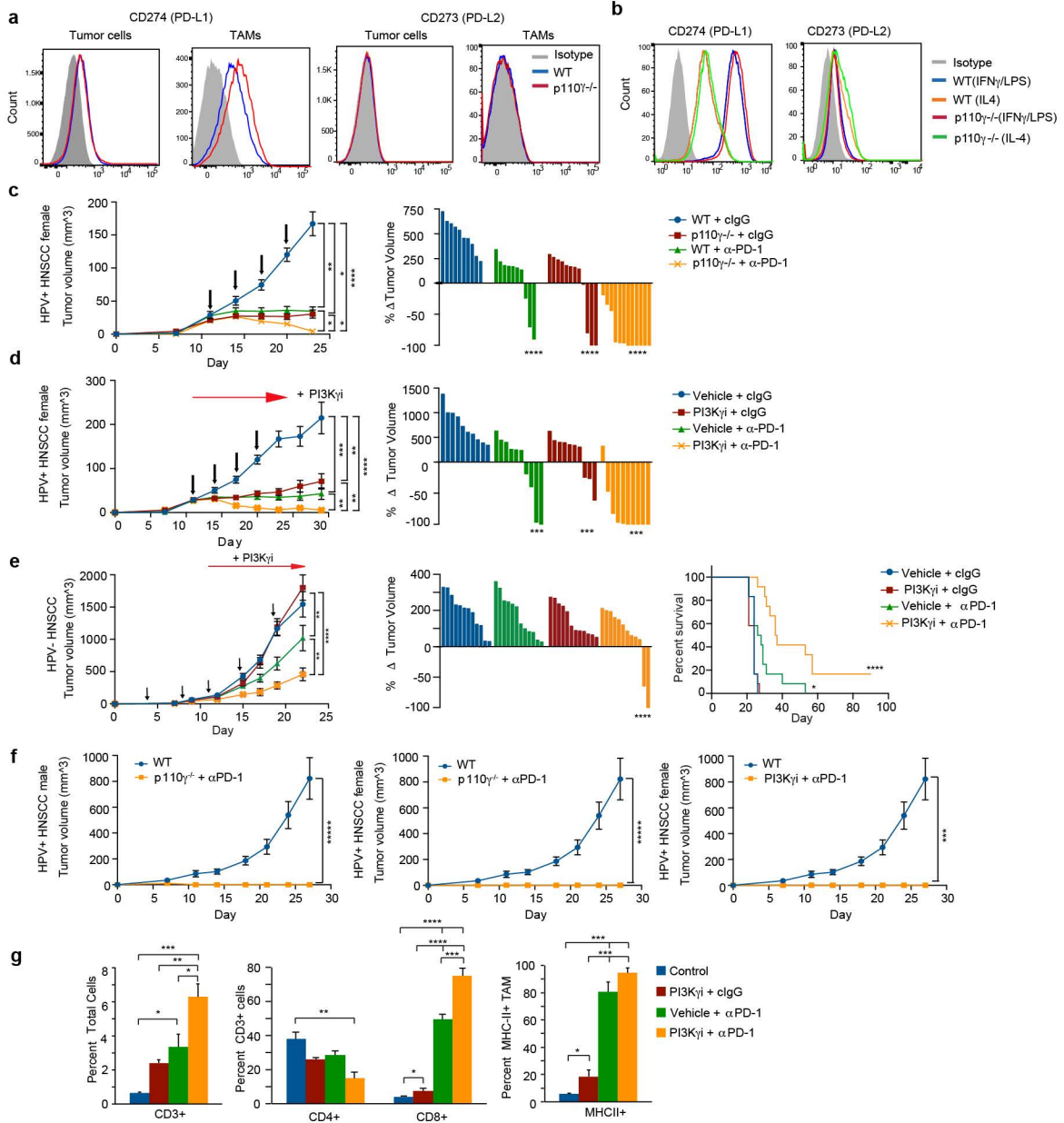




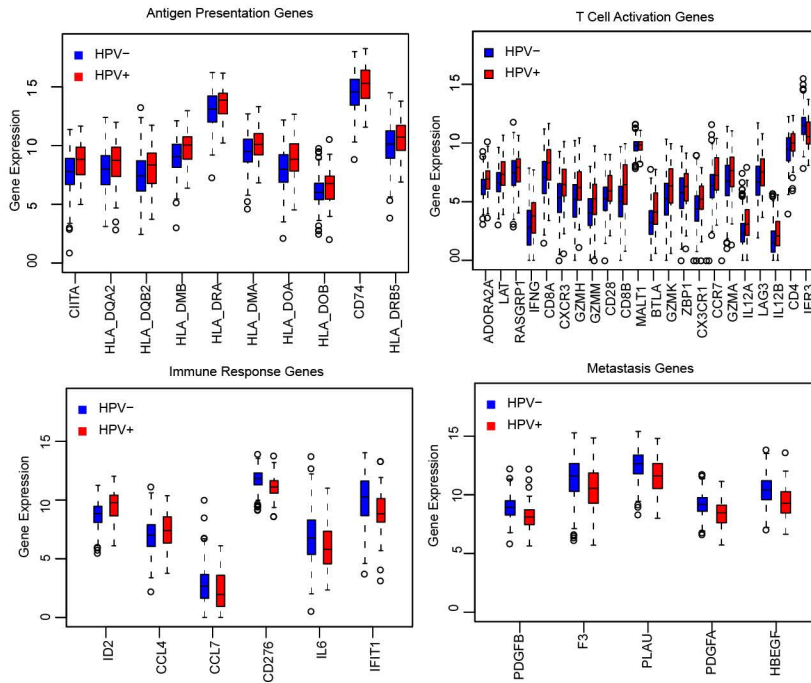




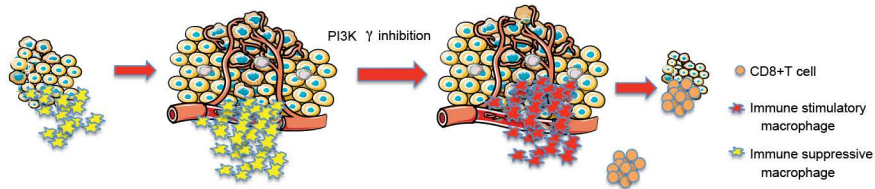




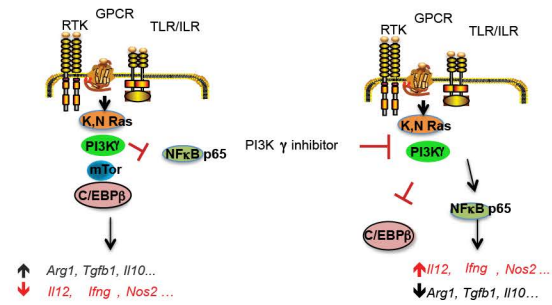
a

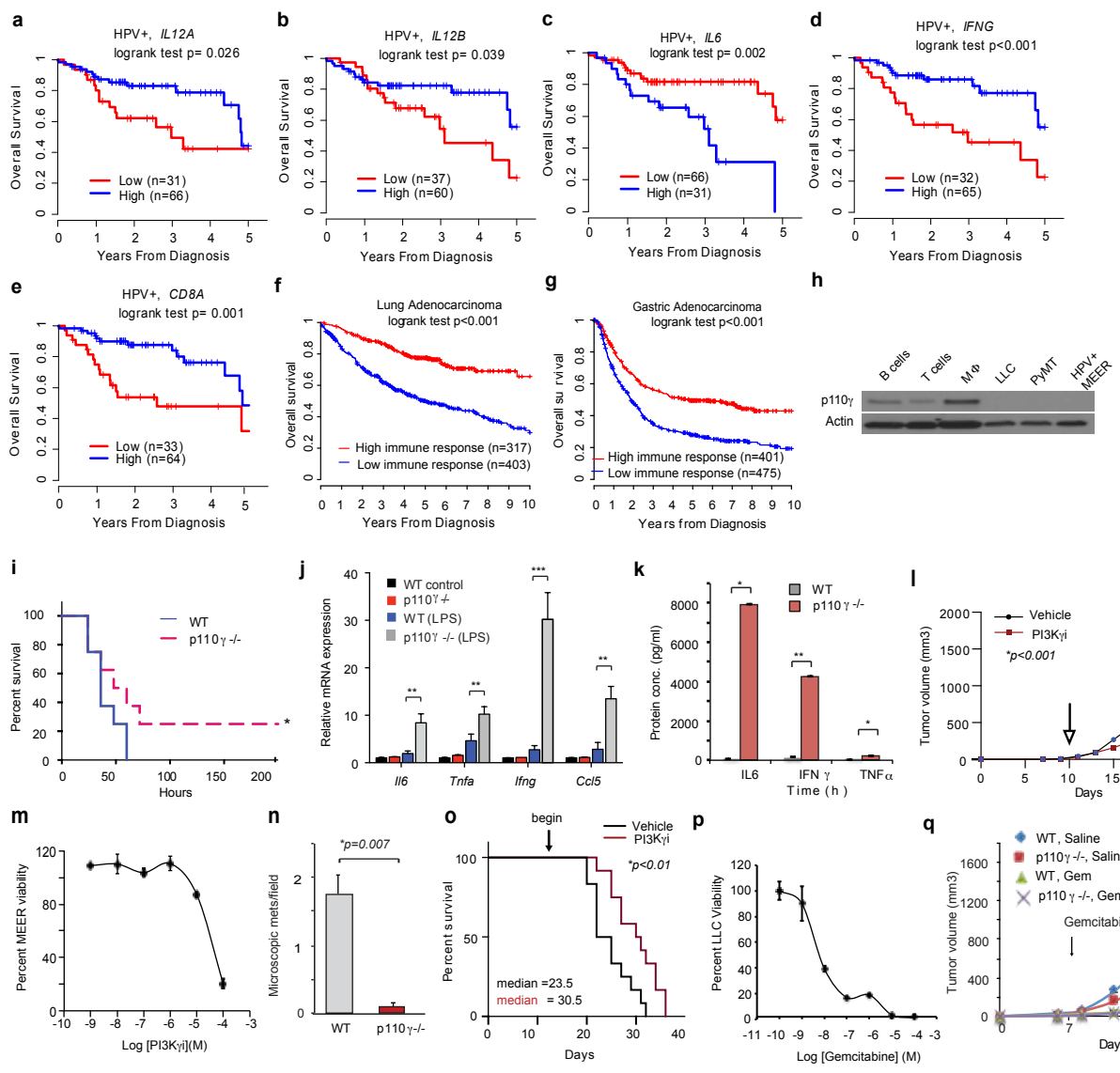


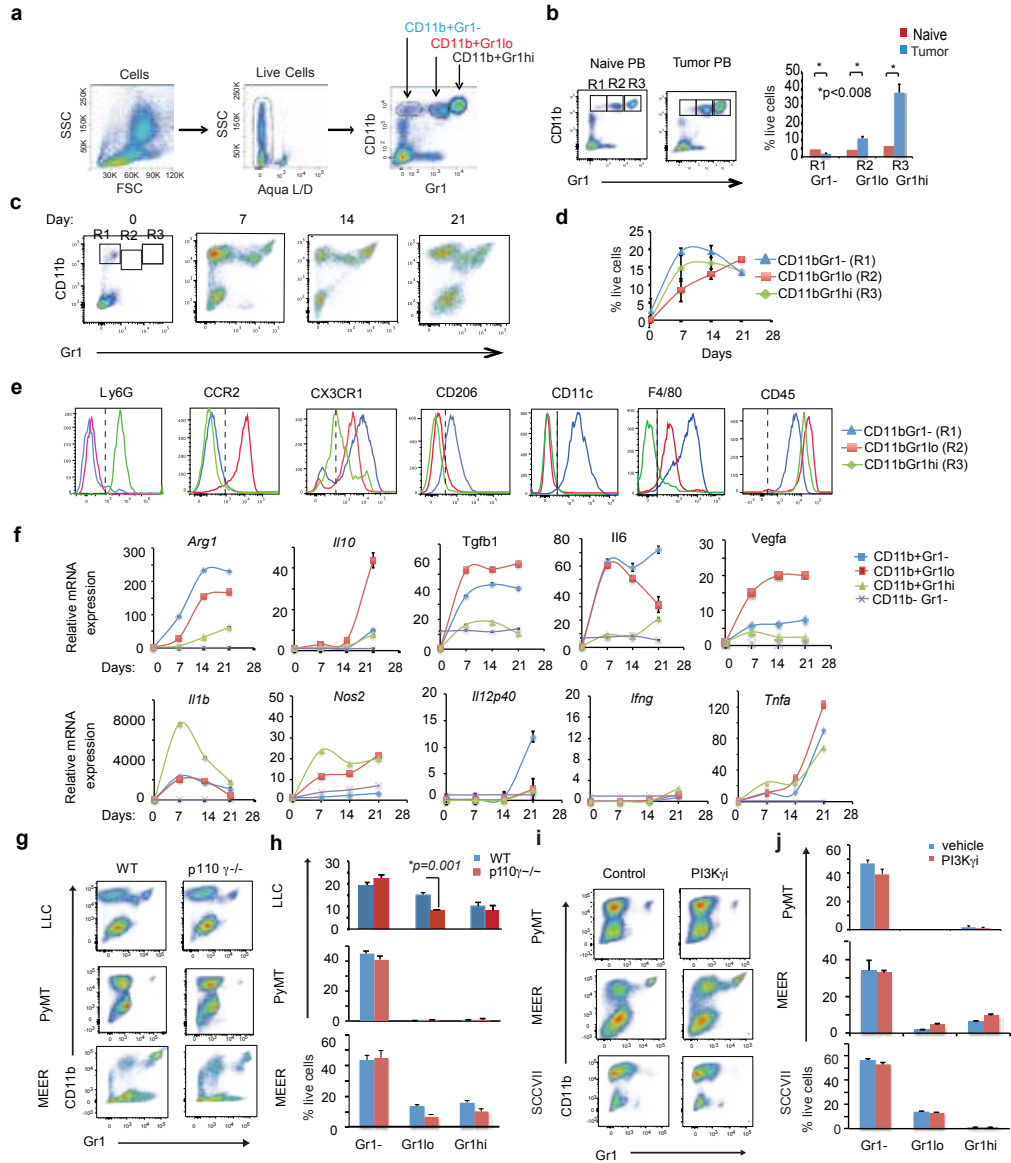
b

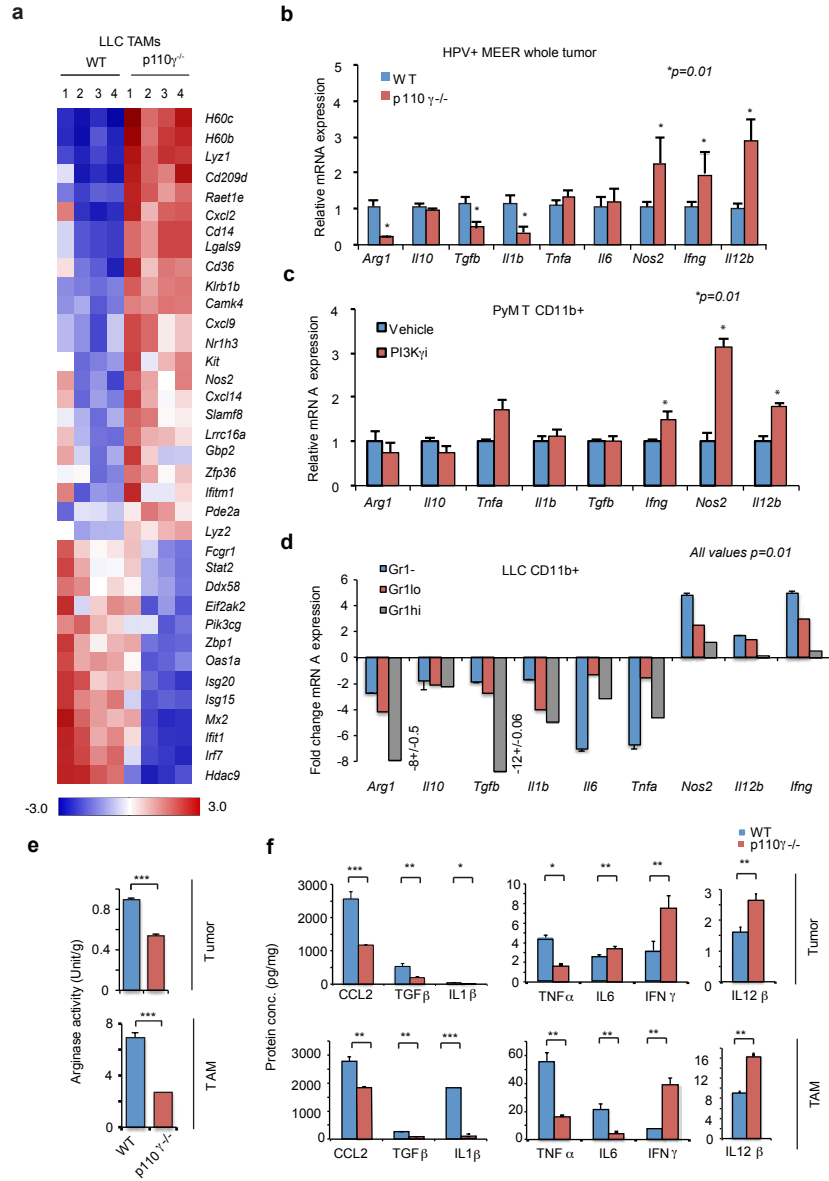


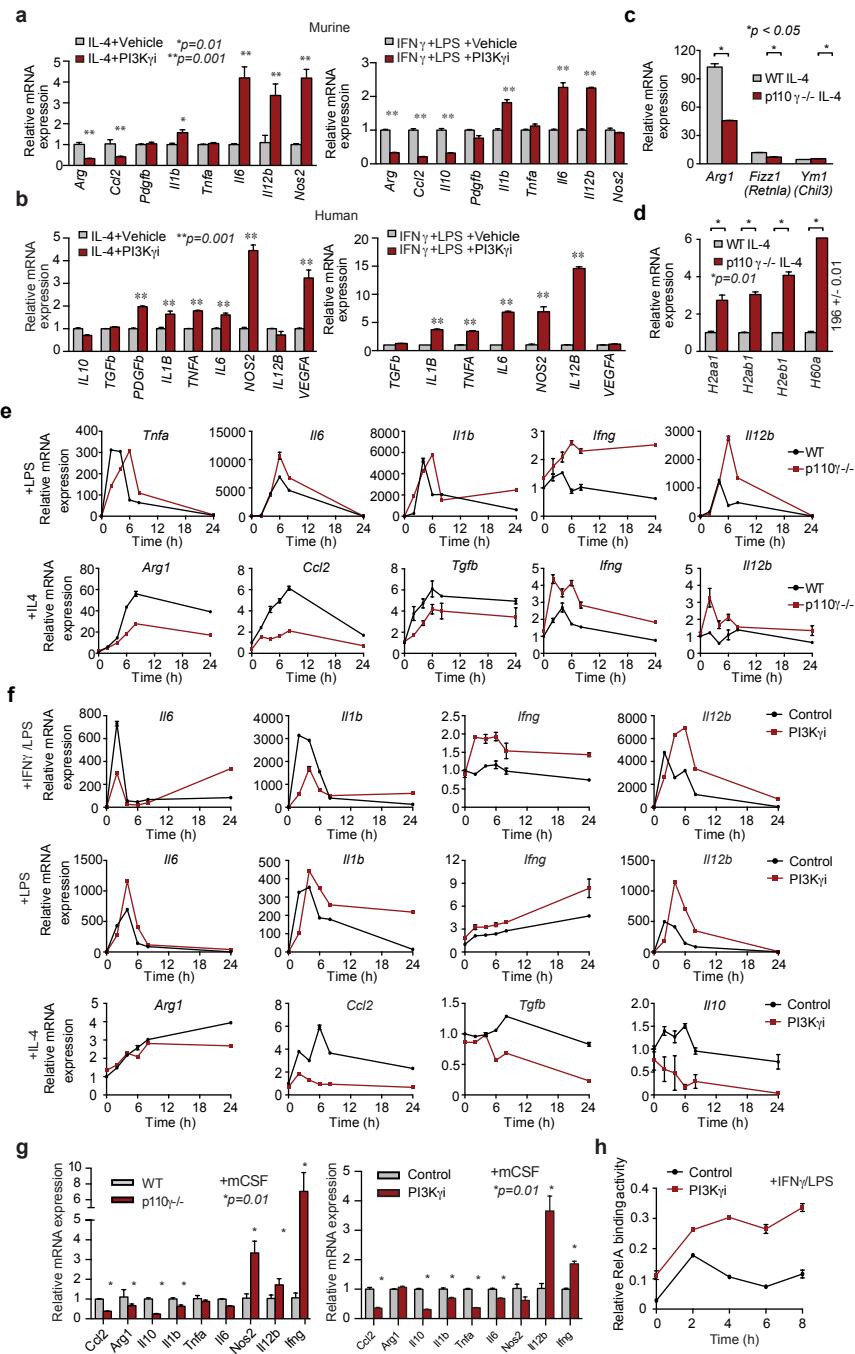
c

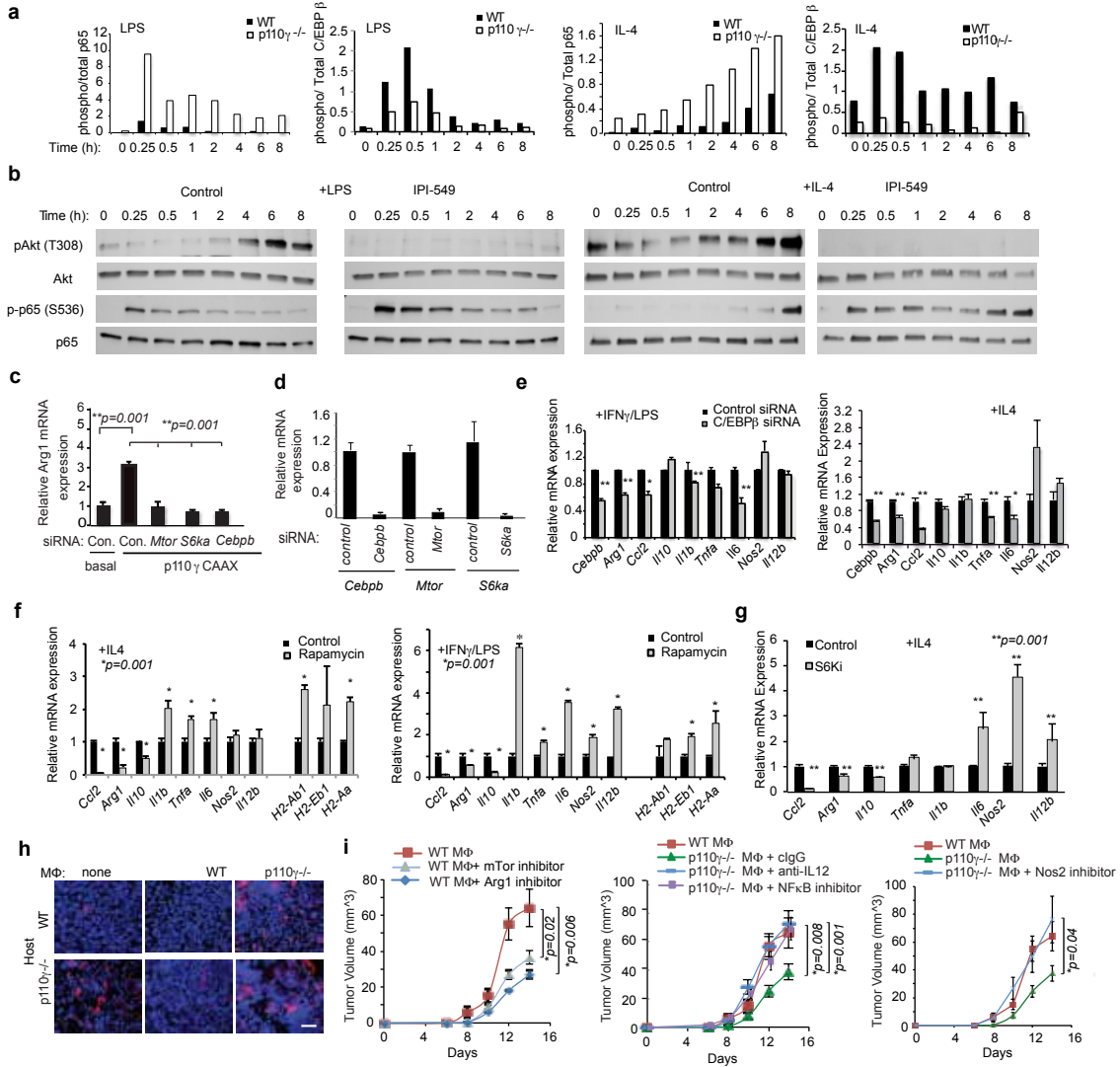


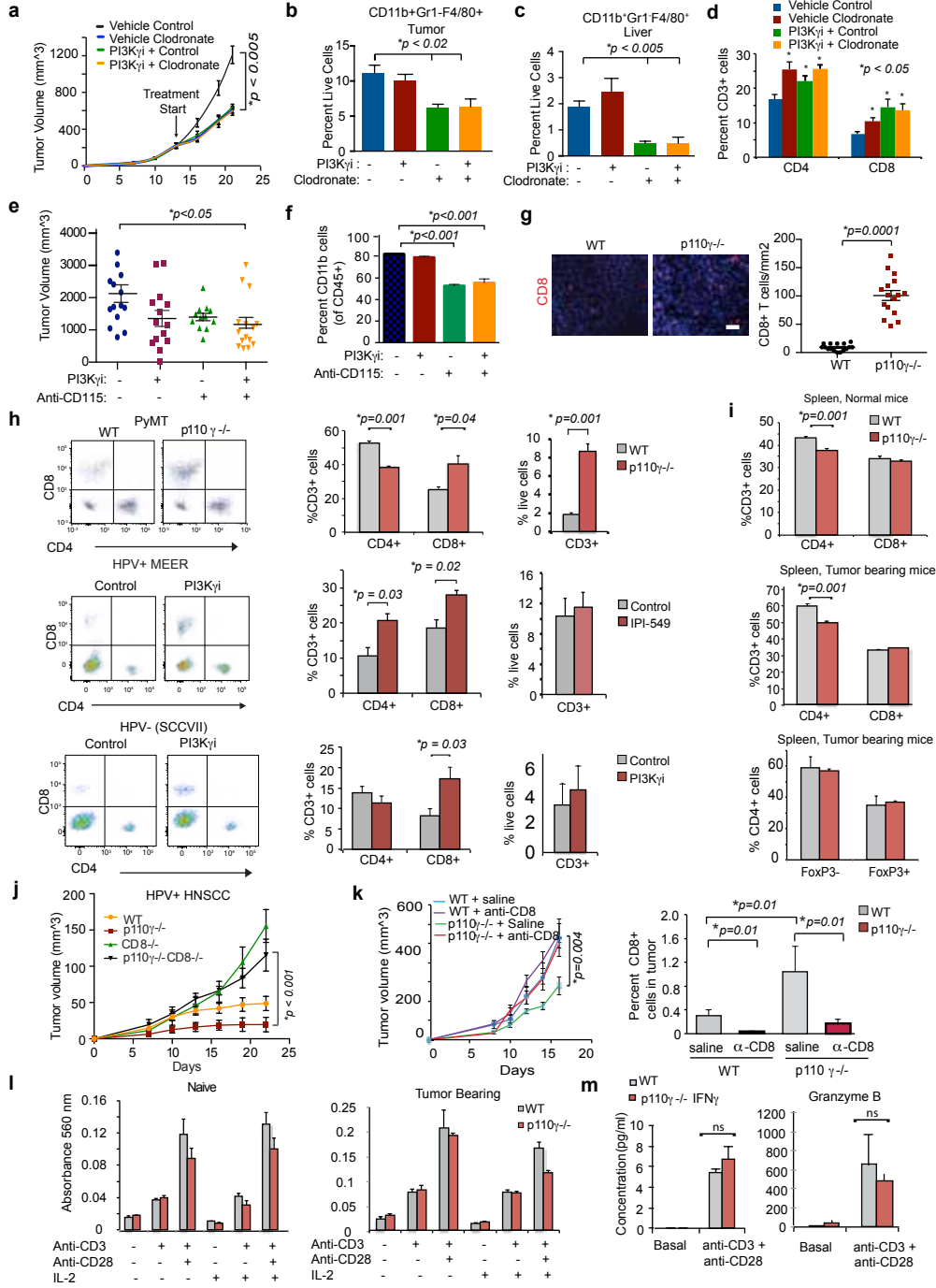


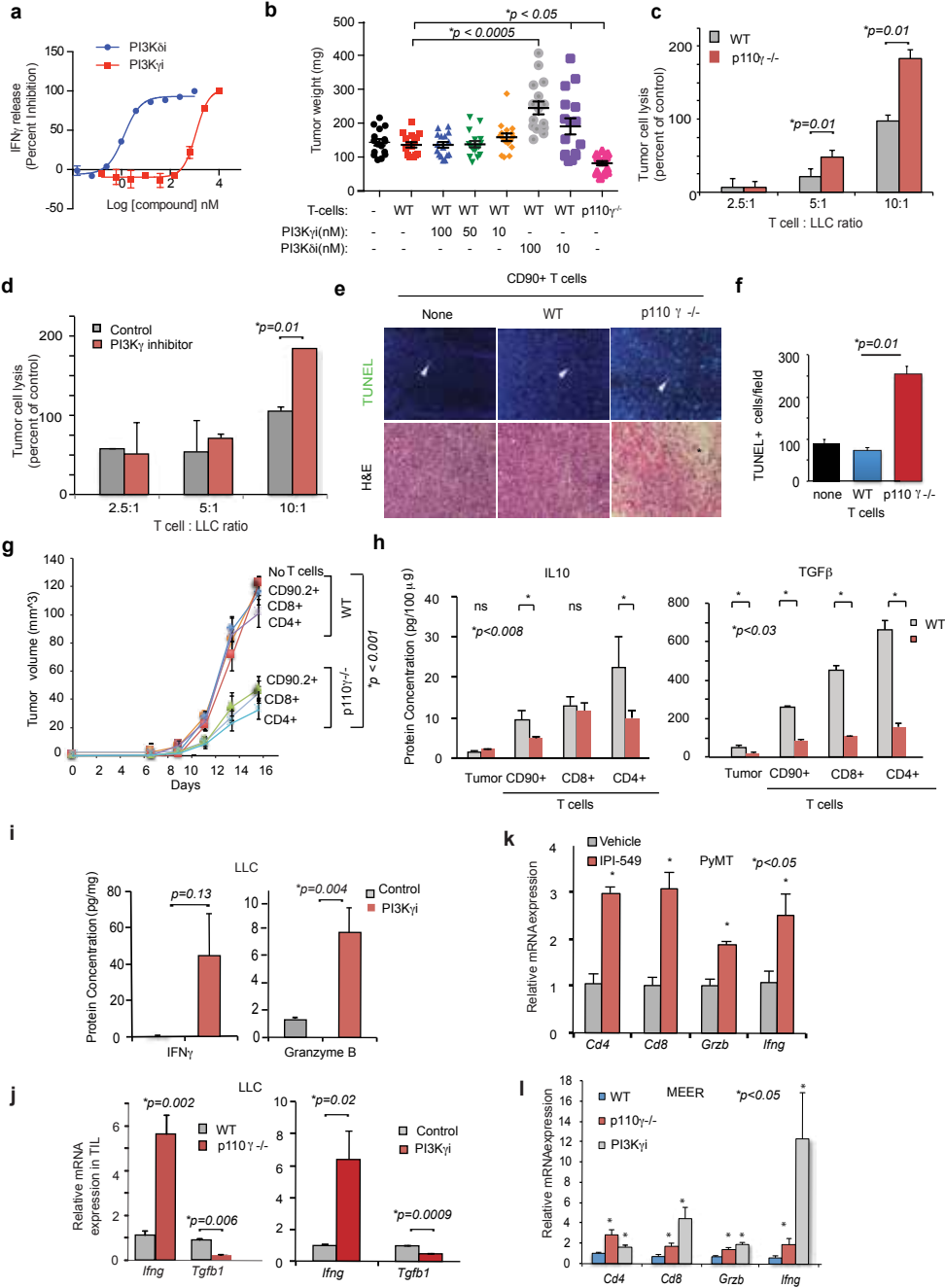


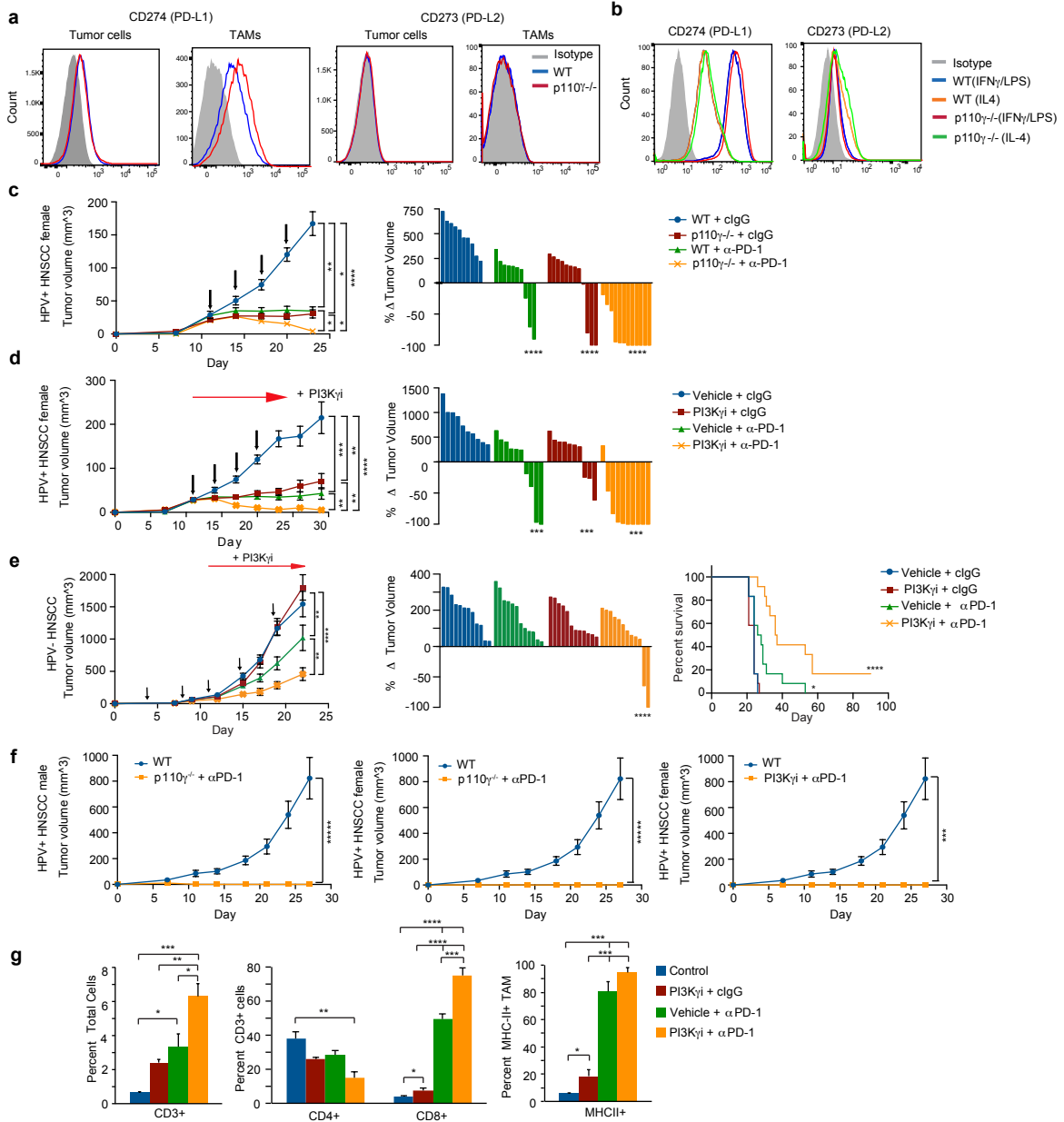




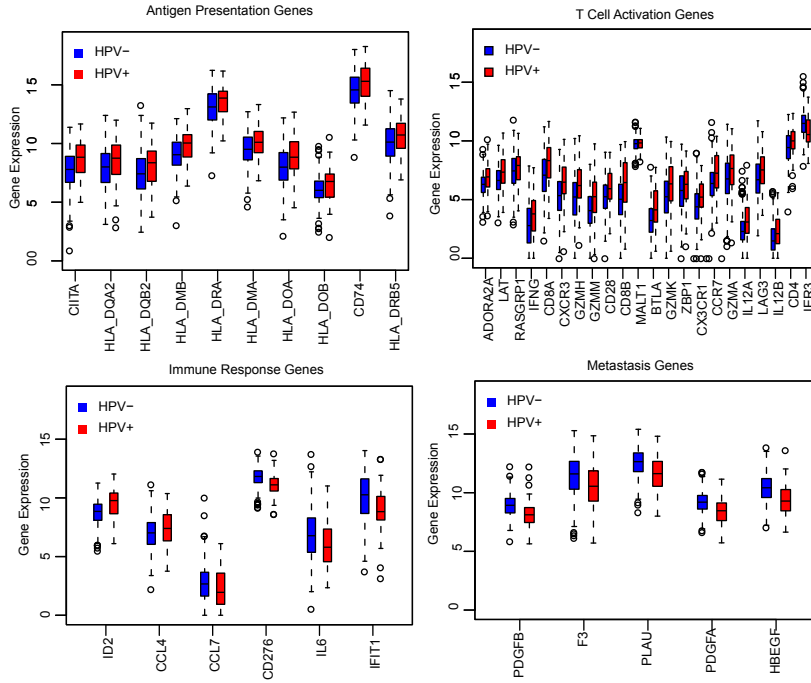




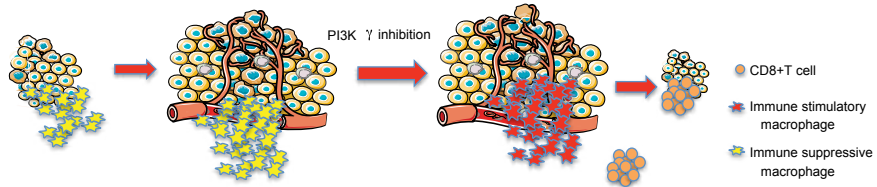




a



b



c

